PET radiomics in lung cancer: advances and translational challenges

Yongbai Zhang[1†], Wenpeng Huang[1†], Hao Jiao[1] and Lei Kang[1*]

†Yongbai Zhang and Wenpeng Huang contributed equally to this work.

*Correspondence:
Lei Kang
kanglei@bjmu.edu.cn
[1]Department of Nuclear Medicine, Peking University First Hospital, No. 8 Xishiku Str., Xicheng Dist, Beijing 100034, China

Abstract

Radiomics is an emerging field of medical imaging that aims at improving the accuracy of diagnosis, prognosis, treatment planning and monitoring non-invasively through the automated or semi-automated quantitative analysis of high-dimensional image features. Specifically in the field of nuclear medicine, radiomics utilizes imaging methods such as positron emission tomography (PET) and single photon emission computed tomography (SPECT) to evaluate biomarkers related to metabolism, blood flow, cellular activity and some biological pathways. Lung cancer ranks among the leading causes of cancer-related deaths globally, and radiomics analysis has shown great potential in guiding individualized therapy, assessing treatment response, and predicting clinical outcomes. In this review, we summarize the current state-of-the-art radiomics progress in lung cancer, highlighting the potential benefits and existing limitations of this approach. The radiomics workflow was introduced first including image acquisition, segmentation, feature extraction, and model building. Then the published literatures were described about radiomics-based prediction models for lung cancer diagnosis, differentiation, prognosis and efficacy evaluation. Finally, we discuss current challenges and provide insights into future directions and potential opportunities for integrating radiomics into routine clinical practice.

Keywords Radiomics, Nuclear medicine imaging, Position emission tomography, Single photon emission computed tomography, Lung cancer, Clinical translation, Cancer imaging

Background

Lung cancer remains a significant global public health concern, characterized by a high incidence and mortality rate, and is recognized as a leading cause of cancer death [1–3]. In 2022, there are estimated 236,740 new cases of lung and bronchial cancer diagnosed, and 130,180 related deaths in United States [2]. Despite huge progress in screening, diagnosing and treating lung cancer, it remains a serious health issue that demands continued attention and researches [4, 5].

These years, imaging has gained more importance in clinical practice for disease detection, diagnosis, staging and treatment monitoring, especially since the concept of personalized precision medicine was put forward [6, 7]. Nuclear medicine imaging (NMI),

mainly comprising of single photon emission computed tomography (SPECT) and positron emission tomography (PET), represents one of the most vigorously evolving imaging modalities [8]. With the prominent advantage of showing anatomical positions and functional conditions simultaneously, the quantitative technique, PET combined with CT, has been widely introduced in imaging, remarkably in oncologic imaging [9]. 2-Deoxy-2-[fluorine-18]-fluoro-D-glucose (^{18}F-FDG) PET/CT has been proven to be an important tool for the detection, identification, and staging of non-small cell lung cancer (NSCLC), the predominant type of lung cancer, demonstrating evident superiority over conventional anatomy-based imaging modalities [10]. It can detect distant metastases and mediastinal lymph node involvement with higher sensitivity and specificity and help guide treatment decisions. While the utility of PET in small cell lung cancer (SCLC) remains debated due to the potential for false-positive metastases detected on PET scans, the European Society for Medical Oncology (ESMO) guidelines recommend the use of PET/CT to aid in radiation therapy volume delineation for this aggressive cancer type [11]. However, the prone bias influenced by multiple factors such as tumor heterogeneity, image noise, segmentation algorithms and so on during repeated measurements, and unestablished interpretation criteria in many diseases of PET metrics remain to be problems worthy further studying [12, 13].

Radiomics, of which the concept was first brought up by Lambin et al. in 2012 [14], is considered to improve the imaging analysis as an advanced computer vision technique, that can maximize the imaging features extracted from radiologic imaging instruments [15]. Radiomics consists of the high-throughput extraction processes of considerable quantitative imaging features associated with both phenotype and microenvironment of tumor, that are attained by medical imaging modalities [7, 14]. Imaging mining exhibits an encouraging potential for improving the non-invasive diagnosis, characterization, prognosis and treatment planning [16]. It allows for detection of whole tumor despite of its spatial heterogeneity and as well treatment monitoring over time [17]. What's more, it has been demonstrated that some specific imaging traits are linked with sub-visual information about pathogenesis of diseases and even the underlying genotypic alterations which could determine tumor growth patterns and therapy response, and sequentially guide the choice of treatment strategies.

NMI radiomics in lung cancer has gained increasing interest these years. Many studies have been conducted to develop predictive models derived from PET or SPECT images for detection and diagnosis, histological and molecular subtyping, evaluation of treatment response, and prognostication of disease outcomes. The available studies of nuclear medicine radiomics in lung cancer are summarized in Table 1. However, while radiomics holds great promise in improving lung cancer management, challenges and obstacles persist such as the lack of standardization, limited validation and integration with clinical data. Further research and collaborative efforts are necessary to address the remaining hurdles in its translation from bench to bedside. In this review, we summarize the current state-of-the-art radiomics progress in lung cancer, highlighting the potential benefits and existing limitations of this approach. Firstly, we introduce the radiomics workflow, including image acquisition, segmentation, feature extraction, and model building. Then we review the published literature on radiomics-based prediction models for lung cancer diagnosis, differentiation, prognosis and efficacy evaluation. In the end,

Table 1 Summary of studies using PET-based radiomics for lung cancer

Author	Imaging	Aim	Cohort size	Study population	Validation (Available or Not Available)	Outcome comparison	Results
Diagnosis and typing							
Hu et al. (98)	^{18}F-FDG PET/CT	Distinguishing solitary ADC from tuberculosis	n = 235 (163 for training and 72 for validation)	ADC (n = 131) or tuberculosis (n = 104)	A	discrimination between ADC and tuberculosis	The AUC of the RF model was significantly higher than that of the clinical model and was slightly lower than that of the combined complex model
Zhang et al. (99)	^{18}F-FDG PET	Distinguishing tuberculosis nodules from lung cancer	n = 174	tuberculosis nodules (n = 77) or lung cancer (n = 97)	NA	discrimination between tuberculosis nodules and lung cancer	The integrated model was found to be the best classification model
Zhang et al. (100)	^{18}F-FDG PET	Distinguishing ADC from SCC	n = 255(70% for training/validation and 30% for testing)	NSCLC	A	discrimination between ADC and SCC	the logistic regression classifier exhibited the most effective performance
Ji et al. (103)	^{18}F-FDG PET	Distinguishing ADC from SCC in different stages	n = 416 (253 for training and 163 validation)	stage I to III NSCLC patients diagnosed with ADC or SCC	A	discrimination between ADC and SCC	The AUCs of RF model for I to III stage in both the training and validation cohorts were good and the radiomic-clinical nomogram outperformed with higher AUCs
Zheng et al. (104)	^{18}F-FDG PET	Distinguishing benign and malignant SPN	n = 190 (70% for training/validation and 30% for testing)	SPN	A	discrimination between benign and malignant SPN	The combined effect is superior to qualitative diagnoses with CT or PET radiomics models alone.
Salıhoğlu et al. (105)	^{18}F-FDG PET/CT	distinguishing between benign and malignant SPN	n = 48 (70% for training/validation and 30% for testing)	SPN	A	discrimination between benign and malignant SPN	The models provided reasonable performance for the differential diagnosis of SPNs (AUCs ~ 0.81)
Wang et al. (107)	^{18}F-FDG PET/CT	predicting for LVI of NSCLC	n = 148 (70% for training/validation and 30% for testing)	NSCLC	A	Predicting LVI in NSCLC patients	The integrated model was found to be the best classification model
Zheng et al. (108)	[18]F FDG-PET/CT	predicting for brain metastasis of NSCLC	n = 203 (70% for training/validation and 30% for testing)	NSCLC	A	Predicting brain metastasis in NSCLC patients	The C-indices of the RF model in the training, internal validation, and external validation cohorts were 0.911, 0.825 and 0.800, respectively.

Zhang *et al. EJNMMI Physics*   (2024) 11:81

Page 4 of 29

Table 1 (continued)

Author	Imaging	Aim	Cohort size	Study population	Validation (Available or Not Available)	Outcome comparison	Results
Jiang et al. [111]	^{18}F-FDG-PET/CT	assessing PD-L1 expression status in NSCLC	n = 399 (2/3 for training and 1/3 for validation and model evaluation)	stage I-IV NSCLC	A	PD-L1 (SP142) and PD-L1 (28 − 8) expression level over 1% and over 50% prediction	Models based on CT-, PET/CT derived features anticipate PD-L1 expression status relatively accurate, while the CT-based model was superior
Zhang et al. [112]	^{18}F-FDG PET/CT	assessing PD-L1 expression status in NSCLC	n = 58	NSCLC	NA	PD-L1 expression	Heterogeneity-related ^{18}F-FDG PET and CT radiomic features, GLRLM_LGRE and GLZLM_SZE, could predict PD-L1 expression
Li et al. [113]	^{18}F-FDG PET/CT	assessing PD-L1 expression status in NSCLC	n = 136 (70% for training/validation and 30% for testing)	NSCLC	A	PD-L1 expression	the AUC of the fusion model was also higher than that of the RF model and the deep learning model
Liu et al. [120]	^{18}F-FDG PET/CT	identifying the specific EGFR mutation subtypes in ADC	n = 148 (111 for training and 37 for testing)	ADC	NA	specific EGFR mutation subtypes including EGFR-19-MT amd EGFR-21-MT)	The predictive features achieved AUCs of 0.77 for EGFR-19-MT, 0.92 for EGFR-21-MT and 0.87 for the combined EGFR mutation positivity
Li et al. [121]	^{18}F-FDG PET/CT	identifying the EGFR mutation status in NSCLC	n = 115	NSCLC	NA	recognition of EGFR mutation	PET/CT based RFs achieved an AUC of 0.805 for discriminating between EGFR-MT and EGFR-WT
Zhao et al. [122]	^{18}F-FDG PET/CT	identifying the EGFR mutation status in ADC	n = 88 (65 for training and 23 for validation)	ADC	A	recognition of EGFR mutation	The model based on RFs combined with clinical factors achieved best discriminative performance with a AUC of 0.864
Yang et al. [123]	^{18}F-FDG PET/CT	identifying the EGFR mutation status and specific subtypes and predicting the survival benefit of targeted TKIs therapy in NSCLC	n = 313 (70% for training and 30% for validation)	NSCLC	A	specific EGFR mutation subtypes including EGFR-19-MT amd EGFR-21-MT; OS; PFS	Radiomics models exhibited excellent ability to distinguish between EGFR-WT, EGFR-19-MT and EGFR-21-MT; the integrated nomogram was superior to the clinical nomogram and the radiomics nomogram, with C-indexes of 0.80 in the training set and 0.83 in the validation set
Yang et al. [124]	^{18}F-FDG PET/CT	Identifying the EGFR mutation status in ADC	n = 174 (139 for training and 35 for validation)	ADC	A	recognition of EGFR mutation; OS	The model achieved AUC of 0.77 in mutant/wild-type model and of 0.82 in 19/21 mutation site model; the multivariate CPH model achieved a C-index of 0.757

Table 1 (continued)

Author	Imaging	Aim	Study population	Cohort size	Validation (Available or Not Available)	Outcome comparison	Results
Wang et al.(128)	^{18}F–FDG PET/CT	Identifying KRAS mutation status in NSCLC	NSCLC	n = 180 (180 for training and 78 for validation)	A	recognition of KRAS mutation	Integrating EGFR mutation information into the PET/CT RS model elevated the AUC, sensitivity, specificity, and accuracy.
Bourbonne et al.(129)	^{18}F–FDG PET/CT	Identifying KEAP1/NFE2L2 mutation status in NSCLC	NSCLC	n = 432 (158 for training and 274 for validation)	A	recognition of KEAP1/NFE2L2 mutation	The model achieved AUC of 0.8 in mutation prediction in the testing cohort and a hazard ratio of 2.61 in LR risk stratification.
Sanduleanu et al. (134)	[18]FDG- PET/CT	Identifying hypoxia	patients with solid tumors	n = 808	NA	recognition of hypoxic sites	Both disease-agnostic and lung-specific models achieved reasonable AUCs
Prognosis and efficacy evaluation							
Li et al. (138)	^{18}F–FDG PET/CT	predicting the death and recurrent risk in ADC	patients with ADC	n = 752 (including 4 gene expression datasets and 2 ^{18}F-FDG PET image datasets)	NA	OS and RFS	The radiomic signature reflecting biological processes in tumors was significantly associated with patients' OS and RFS (OS: log-rank P = 0.0006; RFS: log-rank P = 0.0013)
Chen et al. (139)	^{18}F–FDG PET/CT	predicting survival in ADC patients receiving targeted TKI treatment	stage III-IV ADC patients receiving targeted TKI treatment	n = 51	NA	OS and PFS	A scoring system combining PET radiomics with clinical risk factors improved survival stratification
Yang et al. (144)	^{18}F–FDG PET/CT	predicting pCR to neoadjuvant chemoimmuno-therapy in NSCLC	NSCLC	n = 185	A	pathological complete response	The integrated model was found to be the best classification model
Nemoto et al. (146)	^{18}F–FDG PET/CT	predicting recurrence after SBRT	NSCLC	n = 82	NA	local recurrence, regional lymph node metastasis, and distant metastasis	the model combining PET imaging features and SVM would be useful in predicting local and regional lymph node recurrence
Krarup et al. (148)	^{18}F–FDG PET/CT	predicting survival	NSCLC patients receiving definitive chemoradiotherapy	n = 233	NA	PFS	The pre-selected RFs were insignificant in predicting PFS in combination with GTV, clinical stage and histology

Table 1 (continued)

Author	Imaging	Aim	Cohort size	Study population	Validation (Available or Not Available)	Outcome comparison	Results
Kirienko et al. (150)	18F-FDG PET/CT	predicting DFS for patients undergoing surgery in NSCLC	n = 295	NSCLC patients diagnosed with ADC or SCC	NA	DFS	The Cox models based on CT, PET, and PET/CT RFs achieved AUCs of 0.75, 0.68, and 0.68, respectively
Ouyang et al. (155)	18F-FDG PET/CT	identifying metastatic LNs from the hypermetabolic mediastinal-hilar LNs in NSCLC	LN = 288 (159 LNs for training and 129 LNs for validation)	NSCLC patients with hypermetabolic LNs	A	recognition of metastatic LNs	PET/CT based model achieved the optimal AUC of 0.874
Sepehri et al. (156)	18F-FDG PET/CT	evaluating the potential benefit of combining different algorithms into a consensus for survival prediction	n = 138 (87 for training and validation and 51 for testing)	stage II and III NSCLC receiving curative (chemo) radiotherapy	A	median OS or OS shorter than 6 months	A consensus of machine learning algorithms could improve prognostic performance

ADC, lung adenocarcinoma; AUC, area under the curve; RF, radiomics feature; NSCLC, non-small cell lung cancer; SBRT, stereotactic body radiotherapy; SCC, squamous cell carcinoma; SPN, solitary pulmonary nodules; EGFR, epidermal growth factor receptor; LVI, lymphovascular invasion; MT, mutant type; WT, wild type; OS, overall survival; pCR, pathological complete response; PFS, progression-free survival; C-index, concordance index; CPH, Cox proportional hazard; RFS, recurrence-free survival; GTV, gross tumor volume; DFS, disease-free survival; LN, lymph node; A, available; NA, not available

we discuss current challenges and provide insights into future directions and potential opportunities for integrating radiomics into routine clinical practice.

Radiomics workflow

The workflow of radiomics can be divided into four main steps (Fig. 1): (1) medical image acquisition and reconstruction; (2) regions of interest segmentation; (3) feature extraction and selection; and (4) model building and validation. Each step contributes to building a reliable and accurate predictive model. By understanding each step in detail, researchers and clinicians can better utilize radiomics to improve clinical decision.

Medical image acquisition and reconstruction

Radiomics features (RFs) we extracted from medical images are supposed to measure tumor heterogeneity without unnecessary confounding variability due to nonstandardised imaging protocols, which would introduce bias to the analysis [7, 18, 19]. Some imaging factors are prone to be influenced by the so called scanner or protocol effect, and it's indispensable to harmonize the image acquisition procedures, e.g. patient preparation, scanner difference, imaging parameters and reconstruction settings, especially in multicenter trials [20]. Compared to the radiomics workflows of CT and MR, the PET/CT radiomics workflow faces challenges in accurately co-registering PET metabolic data with CT anatomical data, particularly in the presence of motion artifacts.

It's fundamental for any quantitative features to gain repeatability and reproducibility, and some associations have made efforts to bring up common guidelines for standardized imaging procedures such as the European Association of Nuclear Medicine (EANM) and its Research Ltd. (EARL) ^{18}F-FDG PET/CT accreditation program [21, 22]. EANM tumor imaging guidelines version 2.0 summarized ^{18}F-FDG PET/CT examination procedures including medical history review, patient preparation, PET and CT acquisition protocols and image reconstruction in details to ensure image quality and image harmonisation in multi-center researches [21].

Image reconstruction has been considered as a pivotal process since it would significantly impact the robustness of PET/CT RFs if researchers don't pay attention to the reconstruction schemes, with nearly 99% features inclined to be instable to the variety
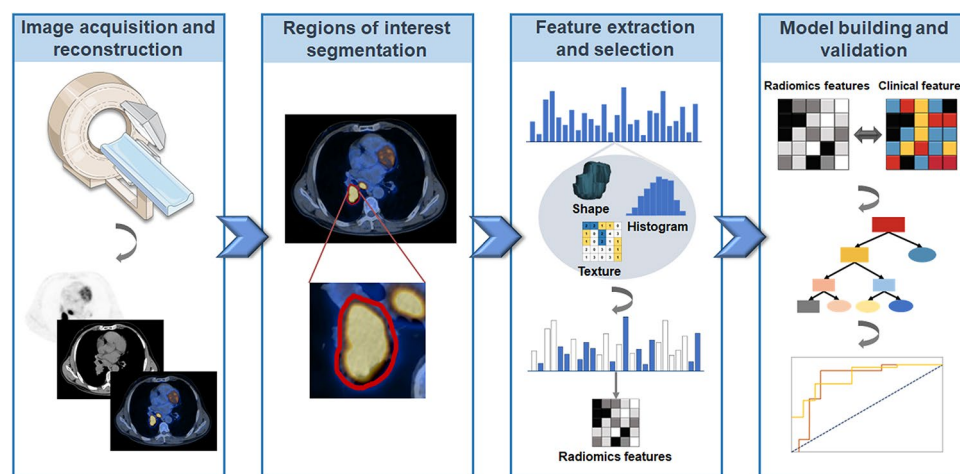

Fig. 1 The pipeline of radiomics research analysis of nuclear medicine. The Figure was partly generated using Servier Medical Art, provided by Servier, licensed under a Creative Commons Attribution 3.0 unported license

of reconstruction algorithms [23, 24]. Pfaehler et al. [25] carried out a multicenter phantom study to compare the feature consistency using different reconstructions that are EARL-compliant or the clinically preferred setting, and found that RFs were more likely to gain a high intraclass correlation coefficient (ICC) with EARL-compliant reconstructions, demonstrating their utility in harmonizing a wide range of imaging traits. And the updated EARL standards (EARL2) are recommended, especially in multicenter settings, as they offer improved contrast recovery and spatial resolution than the earlier EARL1 standards.

Conventional post-reconstruction harmonization procedures such as post-reconstruction filtering can be used to reduce variability between different PET scanners and reconstruction protocols [26]. However, spatial resolution of images could be affected during these postprocessing, that is to the disadvantage of subsequent quantitative and radiomics studies [20]. The ComBat was introduced to deal with batch effects, i.e. the non-biological experimental variation, in researches of gene expression microarrays in the first place [27] and Orlhac et al. [28] determined its efficacy to remove batch effect and harmonize RFs in PET, which could be directly applied to the extracted quantitative features other than the image itself [29]. Recently, Leithner *el al* [30]. conducted a retrospective study including 200 patients to investigate the capacity of ComBat to improve tissue classification accuracy in a pooled PET/CT and PET/MRI radiomics dataset. The results showed ComBat-harmonized group gained higher median accuracies in both train and validation datasets, for various feature classes such as gray-level histogram, gray-level size-zone matrix, and neighborhood gray-tone difference matrix, which suggested ComBat as a promising and recommended tool for the generalization of PET data, especially for technically heterogeneous datasets.

The evolving landscape of PET/CT imaging, such as digital detectors and long axial field-of-view (LFOV) scanners, holds significant potential to impact and refine the current radiomics workflow. These cutting-edge techniques facilitate higher resolution, signal-to-noise ratio and sensitivity, enable faster whole-body acquisitions and concomitantly reduce radiation exposure [31]. Improved quantitative accuracy can provide more reliable and reproducible measurements of radiotracer uptake, benefiting the extraction of quantitative radiomics features. Digital PET/CT, combined with optimal reconstruction algorithms, can significantly reduce image noise and artifacts, yielding cleaner and more accurate images for radiomics analysis [32]. However, the introduction of these new PET/CT technologies necessitate more efforts for the development of standardized protocols to ensure consistent feature extraction across different systems and sites.

Regions of interest segmentation

Delineation of volume of interest (VOI) or region of interest (ROI) influences the determination of voxels to be analyzed and is crucial for the sequent outcome of quantitative feature extraction [33]. Some studies showed less than 20% PET features could be stable with variable segmentation algorithms [34]. Segmentation can be processed manually, semi-automatically or fully automatically [7]. In consideration of the time-consuming and observer-dependent nature of manual segmentation, as well as the high inter-observer variability that can arise, even with the consensus of several experts [35], semi-automatic and automatic methods are more preferable in present radiomics studies for tumor contour delineation [36, 37].

A large quantities of (semi-)automatic segmentation algorithms have been evolved and applied in both pre-clinical and clinical studies and semi-automatic methods are considered to be able to maximize the accuracy while saving time and reducing tedious work [38]. Currently, thresholding-based methods are the most frequent segmentation technique, defining all voxels above a certain threshold as foreground and others as background, of which the optimal threshold is expected to minimize within-class variance or maximize between-class variance [39]. Iterative and adaptive thresholding segmentations are proposed to improve fixed thresholding algorithm, adapting the threshold on the basis of actual images [35]. However, there are many limitations remaining to be tackled for thresholding including inhomogeneity of tumors, motion artefacts, low resolution and inherent noise, making it hard to gain consensus on the threshold value, which will hinder its further application in clinical practice [40, 41]. Matteo et al. [42] used the Dice similarity coefficient to compare automatic segmentation (nnU-Net) with a reference manual segmentation performed by a physician in images of patients with lung tumour. It was found that there was no statistical difference in the accuracy of survival classifiers when using manual and automatic contours, and the results supported the promise of nnU-Net in automatic segmentation.

Other PET segmentation methodologies are identified as region-based, boundary-based, stochastic and learning-based algorithms [41]. Recent years, segmentation methods based on deep-learning (DL) approaches have captured extensive attention for its improved accuracy attributed to their capability to adapt to more complex actual conditions [43, 44]. The Medical Image Computing and Computer Assisted Intervention (MICCAI) challenge carried out the first study that compared the performance of 13 advanced automatic segmentation algorithms on a large dataset and demonstrated DL method using convolutional neural network (CNN) scored the highest median accuracy [45]. One of the most famous CNN based networks, U-Net, initially proposed by Ronneberger et al. [46], could be trained end-to-end from small amount of training images due to data augmentation with elastic deformations, and lots of variations of U-Net have been created to enhance its precision and robustness, for example, the recurrent residual U-Net [47], ICA U-Net [48], dNet [49], and V-Net [50]. Li et al. [51] introduce a technique for multimodality segmentation in PET/CT, leveraging a 3D fully convolutional network (FCN) based on the V-Net architecture for CT segmentation, along with a fuzzy variational model for integration, which could conquer the disadvantages of low spatial resolution and blur tumor edges of PET and enables the combination of PET and CT information to enhance the overall segmentation results. Similarly, Protonotarios et al. [52] proposed a few-shot learning (FSL) strategy integrated into dual-channel U-Net for global-local fused PET/CT image segmentation and illustrated that dual-channel U-Net performed better in terms of F1-score and intersection over union (IoU) than both PET U-Net and CT U-Net. FSL U-Net significantly decreased the error rate of F1-score, IoU, and accuracy compared with original dual-channel U-Net, suggesting its promising potential in clinical practice.

Feature extraction and selection

There are four primary subcategories for the most widely used RFs: statistical features, which include histogram-based and texture-based, shape-based, model-based, and transform-based features [53]. The image biomarker standardization initiative (IBSI),

an independent international collaboration, has taken steps to standardise the extraction of these RFs from acquired imaging. This initiative has established consensus-based nomenclature, definitions and reference values for image features and defined a general radiomics image processing workflow to enhance reproducibility of radiomic studies. The detailed definitions of these RFs have been summarized in the reference manual [54, 55].

Various feature extraction platforms have been constructed by investigators for feature calculation, such as the extensive CERR [56], 3D Slicer [57], PyRadiomics [58], LIFEx [59], RaCaT [60] and CGITA [61]. 3D slicer is a free and powerful open source software for medical image computing and visualization. It supports various image formats, provides tools for image registration, segmentation, and quantitative analysis, and offers a modular architecture, allowing users to extend its function through plugins and extensions, including radiomics extension [57]. PyRadiomics is an open-source Python library for standardised image processing and radiomics quantification. This platform offers two interfaces: a convenient front-end interface in 3D Slicer, and a back-end interface allowing automation in data processing and feature definition. It can extract a comprehensive set of commonly used and IBSI compliant features, supports 2D and 3D segmentations of various imaging modalities and can be easily integrated into existing Python-based workflows and has been widely adopted in radiomics researches [58]. LIFEx is a free, multiplatform software which enables the calculation of histogram-, texture-, and shape-based features and allows characterization of tumor heterogeneity from multimodal imaging data. The platform has been widely used in radiomics studies focused on cancer diagnosis, prognosis, and treatment response prediction [62, 63].

Studies demonstrated that different calculation settings and platform versions had significant impacts on the reliability of RFs and prognostic models [64, 65]. Therefore, researchers should be cautious about the new proposed packages in their research and should publish the unreserved calculation parameters in order that their achievement could be applicable to extensive studies [65]. Meanwhile, additional endeavors need to be taken to standardize feature extraction procedures including feature naming convention, arithmetical definitions and calculation methodologies to ensure consistency and reproducibility in further radiomics studies.

Feature selection is one of the fundamental steps in radiomics workflow. It refers to the process of choosing the most relevant and informative features to analyze from the vast amounts of data generated in medical images. The application of the limitless number of RFs, which are regarded as high-dimensional data, can not only result in the increased cost of data storage and computing time but lead to the model overfitting, making the model "self-assessing" and decreasing in its prediction performance in real-world datasets [7, 66]. Additionally, it's important to select the robust features which are less susceptible to variations in imaging protocols, scanner types, and other technical factors to ensure the reproducibility of radiomics models across different centers and clinical settings. Thus, the most robust, informative and archetypal features with the highest interpatient variability should be selected from a high-dimensional dataset through supervised selection methods or unsupervised ones.

Those methods are mostly based on dimensionality reduction algorithms for the intention of reducing redundancy and elevating accuracy while maintaining the characteristics of original data [53]. Supervised feature selection is usually executed with

users having some prior ground knowledge related directly to a specific clinical problem, especially classification labels such as benign and malignant, while learning from data [67, 68]. Unsupervised methods refers to the algorithms without pre-existing classifications that are expected to automatically create class labels by searching for similarities and grouping pieces of data together [68]. Most commonly used unsupervised methods include the linear category such as principal component analysis (PCA) [69], the non-linear category such as t-distributed stochastic neighbor embedding (t-SNE) [70], multi-dimensional scaling (MDS) [71], and consensus cluster analysis [72].

Each has its own strengths and weaknesses that supervised techniques are more likely to cause overfitting while the unsupervised tend to mix variables and increase the complexity of identifying the original predictors in the initial feature set [53]. Anowar et al. [73] conducted an empirical study comparing performance of 10 dimensionality reduction algorithms in terms of classification accuracy and run-time in three binary and multi-class datasets and observed that all of these algorithms could elevate the data quality and classification accuracy. Nonlinear and manifold-based architectures outperformed linear and random projection-based ones, respectively, in most cases, while as for the multi-class datasets, supervised algorithms surpassed unsupervised. However, there was no definite superior choice and the optimal algorithm could be determined based on the nature and quality of specific datasets. Lian et al. [74] developed extensive feature selection systems based on Dempster-Shafer theory, namely Evidential Feature Selection (EFS), with the improvement of prior knowledge and data balancing, to deal with the uncertain and imprecise information and usually small-sized and imbalanced training samples for prediction of tumor treatment outcome. However, effective feature approaches is often hindered by some similar challenges such as limited sample size, lack of standardization and biological interpretability which should be addressed in future radiomics studies.

The selected features are supposed to be robust to imaging parameters and image processing steps, including scan interpolation which is applied to address image resolution variations [75]. To prevent 3D feature distortion due to anisotropic voxels in routine clinical imaging, resampling images using 3D interpolation with equal resolution in all three dimensions (i.e. $\Delta z = \Delta x = \Delta y$) is recommended [76, 77]. Whybra et al. [77] assessed the stability of 141 texture features to interpolation for a variety of isotropic voxel dimensions, using PET images of 441 esophageal cancer patients and categorized 93 features as stable response, 34 as systematic response that were potentially correctable to a correction model, and 8 as unstable response. And they also observed significant feature value variations when chose different interpolation methods.

Model building and validation

Once the relevant features have been identified, the next step is to train a predictive model that employs these features to identify patterns that are indicative of certain disease outcomes, which could be scalar (e.g., survival time) or categorical (e.g., benign or malignant) [38, 53].

Multiple machine learning (ML) methods are available for constructing models, including logistic regression (LR) [78], support vector machines (SVM) [79], multilayer perceptron (MLP) [80], random forests [81], k-nearest neighbors (kNN) [82], CNN [83], k-means clustering [84, 85], and consensus clustering [86], which could be also classified

into supervised and unsupervised. SVM is one of the most earliest and popular classifiers used in radiomics [38]. It's a supervised algorithm that works by identifying the best possible boundary line, so called hyperplane, to separate data points and maximize the distance between support vectors, that are defined as the nearest examples to the hyperplane [87, 88]. Recently, Choi et al. constructed a predictive radiomics model utilizing SVM combined with absolute shrinkage and selection operator to identify aggressive subtypes of lung adenocarcinoma (ADC). It showcased remarkable performance in terms of categoric precision and accuracy compared with conventional predictor SUV-max [89]. MLP is also a powerful supervised DL algorithm. MLP models the computational units of multiple layers by mimicking signal transmission and this deep neural network architecture helps overcome limitations of getting trapped in local optimal solutions during the training process [80].

Similar to the previous session of feature selection algorithms, supervised and unsupervised classifiers are prone to some disadvantages when implemented in model construction. Though supervised algorithms are more prevalent in radiomics practice, it warrants close consideration of the risk to overfitting and bias which may amplify the original noise, and additionally, the collection of sufficient labeled data sometimes can be difficult and time-consuming [90]. While based on distance metric and without priori variables, unsupervised algorithms tend to result in decreased accuracy [38]. Janghel et al. [91] implemented different classifiers along with the feature extraction architecture, VGG-16 of CNN, to build a model for AD diagnosis and found that SVM, kNN, and linear discriminant classifiers scored highest mean accuracy for fMRI dataset and kNN for PET dataset.

Semi-supervised learning (SSL) algorithms merge large number of unlabeled data, which is easily obtainable, with a limited amount of labeled data during the training process, exploiting the strengths of unsupervised learning to enhance the supervised model, while also balancing accuracy and lack of sufficient data sources [92]. Much experimentation has been carried out testing the performance of SSL in medical image classification [93]. There is a requirement for additional investigation in its utility in PET imaging considering its limited literature which mainly focuses on AD and MCI neuroimaging [94].

Model validation is an essential step in radiomics researches to ensure the reliability and generalizability of its predictive performance (e.g., discrimination and calibration) and to prevent false optimistic estimate. Internal validation only uses the original dataset and usually incorporates the procedure of dividing a single dataset into training and validation subsets, of which the statistical sampling methods should be reported clearly [7]. Bootstrapping is a classic internal validation approach of which the basic strategy is to resample a bootstrap set (size n) with replacement using the original set (size n) and compare the performance of the bootstrap model and the original model [95]. In cross-validation, original dataset is divided into several subsets and the training and testing subsets are rotated in turns [53]. However, external validation, of which the test data is independent, especially attained from another scanner or institution, is more credible and recommended by researchers and statisticians [96]. Many radiomics models are trained on limited sample size with high-dimensional RFs and powerful deep learning algorithms and this extremely increase the risk of overfitting. External validation using independent datasets is crucial to assess the true generalization performance and

prevent overly optimistic results due to overfitting. Up to now, most radiomics studies lack external validation, significantly limiting the quality and clinical translation [96].

Radiomics application in diagnosis and differentiation in lung cancer

Diagnosis and typing

If diagnoses are made depending on clinical manifestations and imaging examinations, it is possible for some benign lesions to be erroneously identified as lung cancer. Tuberculosis is the common misdiagnosis in areas characterized by a high prevalence of tuberculosis [10, 97]. Hu et al. [98] gathered a retrospective collection of 113 patients with lung cancer and 104 patients with tuberculosis and incorporated PET/CT-based RFs for building a predictive model to differentiate between ADC and tuberculosis. The findings demonstrate that the performance of the PET/CT radiomics model, as measured by the AUC (area under the curve), was significantly superior to that of the clinical model. In addition, compared with the complex model (i.e. the integration of clinical and radiomics model), the radiomics model had a slightly lower AUC in both the training and validation cohorts, though without statistical difference ($P > 0.05$). Zhang et al. [99] aimed to improve the accuracy of differentiating between tuberculosis nodules and lung cancer by applying deep learning techniques. An integrated model that incorporates radiomic features, deep learning outputs, and clinical information was identified as the most effective classification model for diagnosing tuberculosis nodules and solid lung cancer.

In another study, Zhang et al. [100] developed a comprehensive model that combines clinical characteristics with PET/CT imaging features. The results showed that the logistic regression classifier exhibited enhanced predictive accuracy in the validation cohort of the radiomic model. The combined model, with an AUC of 0.870, demonstrated superior predictive capability compared to the clinical model (AUC 0.848) and the radiomics model (AUC 0.774).

The two main histologic subtypes of NSCLC are adenocarcinoma (ADC) and squamous cell carcinoma (SCC), representing roughly 60% and 35%, respectively [101]. There are notable differences in the treatment strategies, prognostic outcomes, and recurrence rates between ADC and SCC [102]. However, CT-guided biopsy poses a huge challenge in cases where lesions are located at a considerable depth within the anatomical structures or adjacent to crucial structures such as bronchia and vasculature. Ji et al. [103] formulated a stage-specific predictive model using PET radiomics that took into account the varying levels of glucose metabolic heterogeneity between different stages of lung ADC and SCC, enabling accurate differentiation between the two lung cancer types. The results found that in both the training and validation cohorts, the radiomics signature performed well for distinction, with AUCs of 0.883 and 0.932, 0.854 and 0.944, and 0.895 and 0.886 for stages I, II, and III NSCLC, respectively. And radiomics-clinical nomograms, which integrated RFs with predictive clinical variables yielded better discriminative performance with higher AUCs across all stages in both cohorts.

Some solitary pulmonary nodules (SPNs), as early indicators of lung cancer, present significant challenges in determining their nature, complicating clinical diagnosis and treatment. The aim of Zheng et al.'s study was to assess the effectiveness of ^{18}F-FDG-PET/CT combined with radiomics in predicting the malignancy probability of SPNs [104]. The area under the ROC curve for the joint, CT, and PET models was 0.929, 0.819,

and 0.833, respectively, in the training group, and 0.844, 0.759, and 0.748 in the testing group. With ongoing advancements in image feature extraction technologies, we can achieve higher classification accuracy, which provides a robust tool for guiding clinical decisions, monitoring, and prognosis.

Salihoğlu et al. [105] utilized ML methods to construct predictive models incorporating ^{18}F-FDG PET/CT-based radiomic factors for the purpose of discriminating malignant solitary pulmonary nodules (SPN) from benign SPN. A retrospective analysis of 48 patients with SPN were conducted, with DL and classical ML algorithms used to build the models. The predictive models exhibited reasonable performance (AUC=0.81) for distinguishing SPNs, with higher sensitivity for the DL model and higher specificity for the classic learning model compared to conventional evaluation. Researchers concluded that PET/CT-based RFs had the potential to enhance the differentiation of SPNs. Lymphovascular invasion (LVI), considered a high-risk pathological feature, significantly increases the incidence of relapse and lymph node metastasis [106]. Wang et al. [107] explored the potential of PET/CT radiomics to predict LVI status and prognosis prior to surgery in patients with early-stage solid lung cancer. A PET/CT radiology nomogram (PET/CT model) was developed for estimating LVI; this model demonstrated notable predictive accuracy in both training (C-index: 0.766; 95% CI: 0.728–0.805) and validation cohorts (C-index: 0.774; 95% CI: 0.702–0.846). To identify independent predictors of brain metastasis, Zheng et al. [108] examined metabolic indicators, CT features, and clinical characteristics in an ^{18}F-FDG PET/CT radiomics model for NSCLC patients. The C-indices for this model in the training, internal validation, and external validation cohorts were 0.911, 0.825, and 0.800, respectively. This model offers physicians a novel approach for screening NSCLC patients at high risk of brain metastasis.

Prediction of therapeutic target expression

Immune checkpoint therapy is currently a hotspot in the clinical practice of NSCLC [109]. It is crucial to develop a new approach to evaluate PD-L1 expression levels and predict the therapeutic efficacy of immune inhibitors. Radiomics may be able to predict immunotherapy response and outcome noninvasively [110]. Jiang et al. [111] included 399 patients with NSCLC and established CT-, PET-, and PET/CT radiomics models based on features obtained from corresponding imaging modality, which had the capability to assess the expression levels of various PD-L1 types. The AUC for predicting PD-L1 (SP142) expression level exceeding 50% were 0.80, 0.65, and 0.77, respectively. In terms of PD-L1 (28−8), the AUC performance score was measured at 0.91, 0.75, and 0.88 across the three types of models. And they concluded PD-L1 expression status could be predicted fairly accurately using radiomics-based predictive methods in NSCLC patients (Fig. 2). In clinical practice, this may help guide immunotherapy. In a retrospective study of 58 NSCLC patients, Zhang et al. [112] analyzed the relationship between presurgery ^{18}F-FDG PET/CT examination and postsurgery PD-L1 expression. The results of multivariate logistic regression analysis revealed that the CT radiomics feature GLZLM_SZE and the PET radiomics feature GLRLM_LGRE were both identified as independent predictors of PD-L1 status. ^{18}F-FDG PET and CT-based RFs related to heterogeneity showed good non-invasive prediction ability for PD-L1. The research by Li et al. [113] underscores the importance of combining radiomics and deep learning to predict PD-L1 expression in NSCLC. The fusion model surpassed both the individual
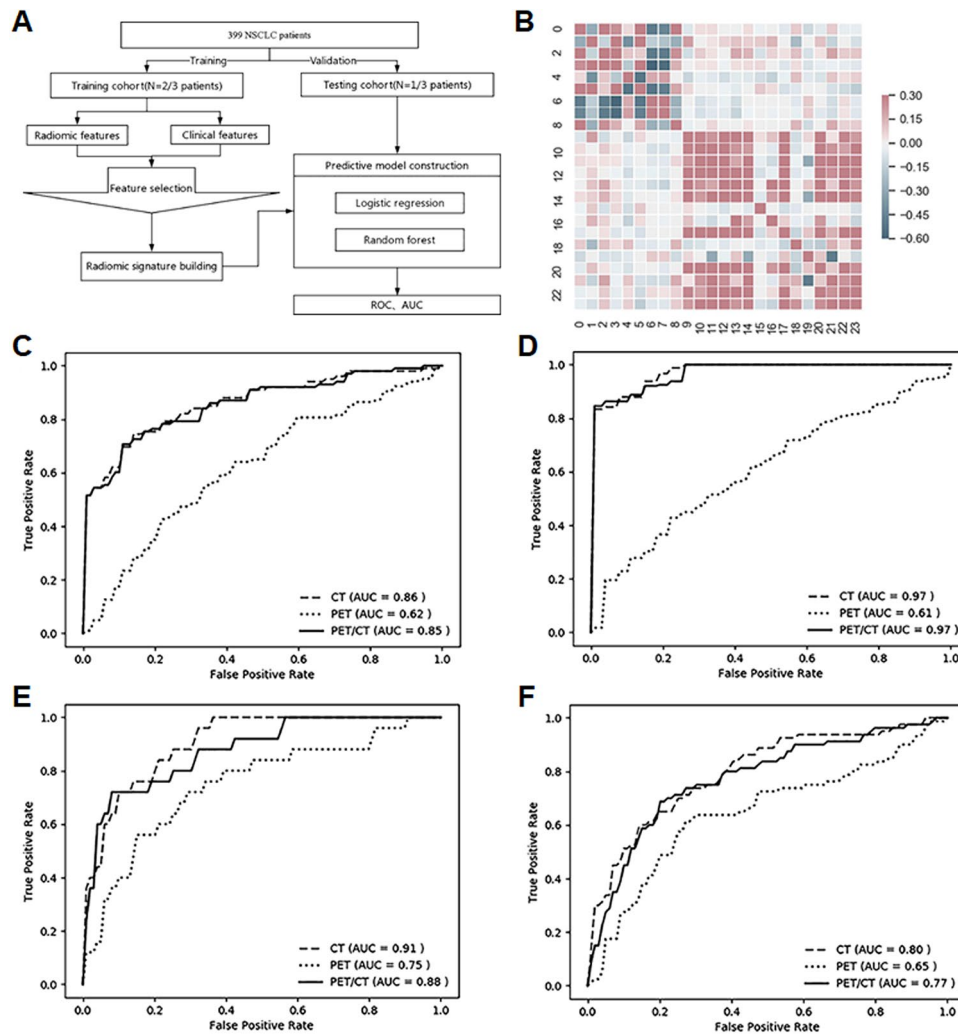
Fig. 2 PET/CT radiomics models for assessing PD-L1 expression level in NSCLC. (**A**) The flowchart of patients. (**B**) Correlation heat-map of the selected feature set. Features numbered 0–11 derived from CT and 12–23 from PET. Classifiers' performance on predicting 1% level of PD-L1 (28 − 8) (**C**), 1% level of PD-L1 (SP142) (**D**), 50% level of PD-L1 (28 − 8) (**E**) and 50% level of PD-L1 (**F**). Data derived from Jiang et al. [111]

radiomics and deep learning models in performance, achieving higher AUC and accuracy, thereby enhancing efficiency. In the training and validation cohorts, the fusion model recorded AUCs of 0.954 and 0.910, respectively.

EGFR mutation status identification

As our understanding of molecular mechanism about lung cancer has advanced, tyrosine kinase inhibitors (TKIs) targeting at epidermal growth factor receptor (EGFR) have gained widespread usage in managing NSCLC [114, 115], and patients harboring EGFR mutations demonstrate significantly prolonged overall survival (OS) and progression-free survival (PFS) in contrast to wild-type EGFR (EGFR-WT) [116, 117]. Therefore, it is vital to detect EGFR mutations before starting targeted therapy with TKIs.

There are two most common subtypes of EGFR mutations in clinical practice: the exon 19 deleterious (E19del) mutation and the exon 21 mis-mutation. After TKI treatment, patients exhibiting E19del mutation possibly experience a superior survival benefit than those harboring the exon 21 mis-mutation, according to increasing evidence [118, 119].

In an analysis of PET/CT images containing ^{18}F-FDG, Liu et al. [120] developed predictive models for lung cancer. The model achieved satisfactory prediction power in identifying the EGFR mutation and its certain mutation subtypes. Two sets of RFs were discovered for predicting the prognosis of distinct subtypes of EGFR mutation including 5 features for E19 deletions and 5 features for E21 L858R mutations. Radiomics prediction accuracy was 0.77 and 0.92, respectively, for both predictors. By combining these two predictors, a model to distinguish positive EGFR mutation could also be constructed, achieving an AUC value of 0.87. Li et al. [121] conducted an integrated study collecting data of 115 NSCLC patients, combining somatic molecular test with PET/CT image, and successfully established a correlation between imaging phenotypes and molecular mutation status. PET/CT-based RFs outperformed individual RFs (the PET radiomics signature, CT radiomics signature, and the common PET parameters such as max standardized uptake value [SUV$_{max}$], SUV$_{mean}$, metabolic tumor volume [MTV], and total lesion glycolysis [TLG]) in discriminating between EGFR-mutant type (EGFR-MT) and EGFR-WT with an AUC of 0.805. To develop robust and comprehensive models, several clinical characteristics that might affect image features, such as age, gender, smoking status, clinical stage, and lesion location, were integrated with radiomics models, with the PET/CT model resulting in an impressive AUC of 0.822. The results of Zhao et al. further supported this view [122]. The retrospective study included 88 patients with ADC and established 4 models based on clinical factors, PET-based RFs, CT-based RFs, and PET/CT-based RFs combined with clinical factors, respectively. The combined model outpaced other prediction models, demonstrating a superior AUC of 0.864 with a specificity of 0.784 and a sensitivity of 0.714. The calibration curve of the nomogram model demonstrated a concordance index (C-index) value of 0.778 in the validation cohort, indicating good clinical utility.

A study by Yang et al. [123] investigated the predictive value of ^{18}F-FDG PET/CT signatures for EGFR mutation profiles, mutation site, and survival with TKI therapy in 313 patients of NSCLC. In multivariate analysis, SUV$_{max}$ was one of the independent predictors for EGFR mutation condition and specific mutation sites. To develop integrated models, 2 clinical factors, 8 CT-based RFs, and 6 PET-based RFs were obtained, which showed excellent ability to distinguish between EGFR-WT, EGFR-19-MT, and EGFR-21-MT. Additionally, researchers conducted a performance comparison of different model construction algorithms and observed that SVM outperformed in the prediction models of the EGFR-WT, EGFR-19-WT, and EGFR-21-WT in both the training and validation cohorts in comparison with the random forest and decision tree models. The integrated nomogram predicts OS better than either the clinical or radiomics nomograms, with C-indexes of 0.80 in the training sets and 0.83 in the validation sets. Improved survival outcomes of NSCLC patients receiving targeted therapy may be achieved through PET/CT-based radiomics model to predict EGFR mutation profiles. Yang et al. [124] retrospectively collected 174 patients diagnosed with ADC over a period of 7 years and found that the combination of ^{18}F-FDG PET/CT-based RFs and several clinical factors had the potential to indicate genetic differences and provide a prediction for prognosis. The mutation status model was evaluated in both the training and validation groups, achieving an AUC of 0.77 and 0.71, respectively. In the training and validation sets, the E19/21-MT model demonstrated an AUC of 0.82 and 0.73, respectively. The multi-factor Cox proportional hazard (CPH) model, which incorporated radiomics

and five clinicopathological variables, demonstrated a C-index of 0.757. Patients with EGFR mutations survived significantly longer with targeted therapy than chemotherapy ($P=0.03$). Nevertheless, the model's generalizability was limited as there was no external validation performed. For further improvement of the research process, a consensus should be reached regarding the harmonization of PET/CT radiomics workflows for predicting EGFR mutation profiles in NSCLC patients [125].

Prediction of alternative pathway

While current research is predominantly centered on the identying mutations of EGFR, it is of great importance to predict other common gene mutations such as KRAS, ROS1 and ALK as patients harboring these gene mutations may benefit from targeted therapies [126]. Previous evidence has demonstrated that KRAS mutation status exhibits association with EGFR mutation status as they manifest a distinct pattern of mutual exclusivity [127]. Wang et al. [128] retrospectively analyzed a dataset of 258 NSCLC patients, including a 180 training cohort and a 78 validation cohort, to investigate whether the mutation exclusion information can optimize the PET/CT radiomics algorithms for predicting KRAS mutation. The composite model which integrated EGFR mutation information into the KRAS PET/CT model exhibited improved accuracy and AUC for predicting KRAS mutations. KEAP1 and/or NFE2L2 mutations also play a crucial role in the pathogenesis and therapeutic resistance of lung cancer. Disruption of the KEAP1-NFE2L2 pathway results in the activation of NRF2, thus promoting the survival, proliferation, and resistance to oxidative stress and chemotherapeutic agents of cancer cells [128]. Additionally, KEAP1- NFE2L2 mutations could be used as biomarkers for prediction of immunotherapy and radiotherapy response in patients with NSCLC [128, 129]. A study conducted by Bourbonne et al. [129] built a PET/CT radiomics model from a 158 patients cohort and validated its effect for predicting KEAP1/NFE2L2 mutation status in 2 cohorts, including an external cohort. The developed model was demonstrated to be able to efficiently identify KEAP1/NFE2L2 mutation and stratify patients at risk of local relapse after radiotherapy.

Dichotomize hypoxic/well-oxygenated tumor evaluation

Radiotherapy and systemic treatment are typically resistant to tumor hypoxia [130]. Hypoxia-indicating methods, such as immunohistology staining utilizing 2-nitroimidazoles, perfusion CT, and various PET imaging agents, including the commonly used ^{18}F-fluoromisonidazole (^{18}F-FMISO), ^{18}F-flortanidazole (^{18}F-HX4), and ^{18}F-fluoroazomycinarabinoside (^{18}F-FAZA), has been widely applied in the determination of the oxygenation status of solid tumors [131−133]. It is assumed that radiomics characteristics derived from CT and FDG-PET can be employed to detect tumors with substantial hypoxia areas. Sanduleanu et al. [134] proposed and validated CT, FDG-PET and PET/CT based radiomics models for hypoxia classification, either agnostic with unknown solid tumor sites or site specific (lung, head and neck [H&N]), and explored the correlation with relevant hypoxia-response genes and the predictive value for OS of these signatures. In three cohorts for external validation, an 11-feature "disease-agnostic CT model" achieved AUCs of 0.78, 0.82, and 0.78. A "disease-agnostic FDG-PET model" achieved an AUC of 0.73 in the validation dataset by combining 5 features. In addition, Kaplan-Meier analysis in an external cohort demonstrated a significant split ($P<0.05$)

in OS between hypoxic and normoxic CT-classification. After correction for multiple testing, 117 significant correlations were found between radiomics features extracted from the $CT_{Agnostic, non-SMOTE}$-signature and hypoxia response genes, demonstrating that both CT- and ^{18}F-FDG PET-based radiomics signatures can properly divide tumor into hypoxic and non-hypoxic groups based on hypoxic fractions cutoffs.

Radiomics application in prognosis and therapeutic efficacy evaluation in lung cancer

Radiomics in surgical planning and prognosis

ADC is a clinically heterogeneous disease and has a high mortality rate, and despite having the same TNM stage, patients may still have widely varying clinical outcomes [135, 136]. Thus, an improved method for predicting death or recurrence risk in ADC patients is necessary. ^{18}F-FDG PET is extensively employed for ADC staging, restaging, and response evaluation [137]. Li et al. [138] analyzed a gene expression dataset containing 334 patients with stage I–IIIA ADC by using a "weighted gene coexpression network analysis" R package to identify a prognostic gene coexpression module, and then developed a noninvasive radiomics signature based on PET-metabolic features that could be individually applied in a clinical setting to recognize patients with ADC who are at an increased risk of death and recurrence. Prognostic capability of the coexpression module with genes enriched in tumor-associated processes such as DNA replication, cell cycle, and p53 signaling pathway was validated and the selected module was sequentially leveraged for extracting a radiomics signature incorporating 3 PET metabolic features. Multivariate Cox regression analysis revealed that the radiomics signature was an independent prognostic factor for OS and recurrence-free survival (RFS) in patients with ADC. Moreover, the radiomics nomograms significantly outperformed the clinicopathological nomograms in terms of concordance index. Chen et al. [139] investigated the prognostic efficacy of ^{18}F-FDG PET RFs in fifty-one patients of EGFR-mutated ADC and treated by targeted TKI. They identified two independent prognostic risk factors associated with decreased OS and PFS, that were high SUV entropy of the primary tumor (>5.36) for radiomics analysis and the presence of pleural effusion for clinical variables and then formulated a score system (ranking from 0 to 2) containing the above items. The new system was found to be superior to the traditional TNM staging system in terms of C-index for OS and PFS and promote survival prognosis stratification in stage III-IV ADC patients. The results may be helpful to optimize individualized treatment strategies.

Radiomics in chemoradiotherapy

A number of semiquantitative FDG PET features, such as the SUV, MTV, and TLG, are associated with particular prognoses in patients with NSCLC [140–142]. Neoadjuvant chemotherapy can decrease tumor size prior to surgery, thereby enhancing the likelihood of a curative resection [143]. Yang et al. [144] aimed to develop and validate a radiomics model using ^{18}F-FDG PET/CT images for predicting the pathological complete response (pCR) to neoadjuvant chemoimmunotherapy in NSCLC patients. The study demonstrated that this PET/CT radiomics model achieved an AUC of 0.818, indicating its effectiveness in forecasting pCR in NSCLC patients undergoing neoadjuvant chemoimmunotherapy. The treatment guidelines for lung cancer recommend

stereotactic body radiation therapy (SBRT) for patients who are medically ineligible for surgery or who opt out of surgical interventions [145]. Nemoto et al. [146] developed and thoroughly assessed models for predicting local, regional, and distant recurrence post-SBRT, utilizing radiomic features and machine learning techniques on PET and CT images. The findings indicate that the model integrating PET imaging features and SVM effectively predicts local and regional lymph node recurrence, while the model incorporating CT imaging features and SVM reliably forecasts distant recurrence. The research conducted by Lucia et al. reached similar conclusions [147].

In an NSCLC patient cohort receiving definitive chemoradiotherapy, Krarup et al. [148] validated the prognostic value of 6 selected RFs extracted from ^{18}F-FDG PET/CT in both univariate and multivariate cox regression analysis, which were jointed with stage, histology and gross tumor volume (GTV) for prognostic assessment. They found that 4 RFs were identified as informative predictors for PFS in the univariate analysis and none in the multivariate analysis, while GTV and clinical stage were observed to be prognostic indicators. They concluded the combined analysis didn't exhibit significant prediction performance and the negative findings was possibly attributed to changes in technical parameters. The stability of RFs is a matter of concern in providing important clinical information. At present, risk evaluation and treatment decision of NSCLC are based on the TNM staging system. There are, however, some limitations to the TNM staging system. For instance, patients with the same stage have varying recurrence rates after curative surgery [149]. A study by Kirienko et al. [150] confirmed the RFs extracted from baseline PET/CT scans could indicate disease-free survival (DFS) in NSCLC patients undergoing surgery. Using Cox models that included RFs for CT, PET, and PET/CT images, the research obtained AUCs of 0.75, 0.68, and 0.68, respectively. As a result of adding clinical predictors (tumor stage) to Cox models, AUCs for CT, PET, and PET/CT images were 0.61, 0.64, and 0.65, respectively (Fig. 3). However, the present study was not able to test smoking habits and differentiation grading because these data were not available for the entire patient cohort. Unfortunately, the findings from Ciarmiello et al. [151] suggest that a radiomic model incorporating tumor stage, SUVmax, and a specific radiomic feature (NGTDM_Coarseness) predicts survival in NSCLC patients as effectively as a reference model consisting solely of tumor stage and SUVmax. The selected radiomic variable did not offer any significant additional value beyond that provided by the tumor stage and SUVmax combination.

Radiomics in lymph node metastasis

Patients with NSCLC will be precluded from receiving primary surgery in the presence of contralateral or multiregional mediastinal-hilar lymph node metastasis, which is significantly predictive of poor clinical prognosis [152, 153]. In recent years, ^{18}F-FDG PET/CT has become a favorable imaging strategy for detecting abnormal lymph nodes [154]. A retrospective study included 259 NSCLC patients who received preoperative ^{18}F-FDG PET/CT scan and were detected with hypermetabolic mediastinal-hilar lymph nodes (LNs) [155]. The researchers developed a PET-based radiomics model to discriminate metastatic LNs from LNs with elevated uptake, and test the model's predictive value in an external dataset. The combined PET/CT model demonstrated excellent discrimination performance for identifying the true metastatic LNs from the hypermetabolic LNs, with an AUC of 0.874, 0.845, and 0.841, respectively.
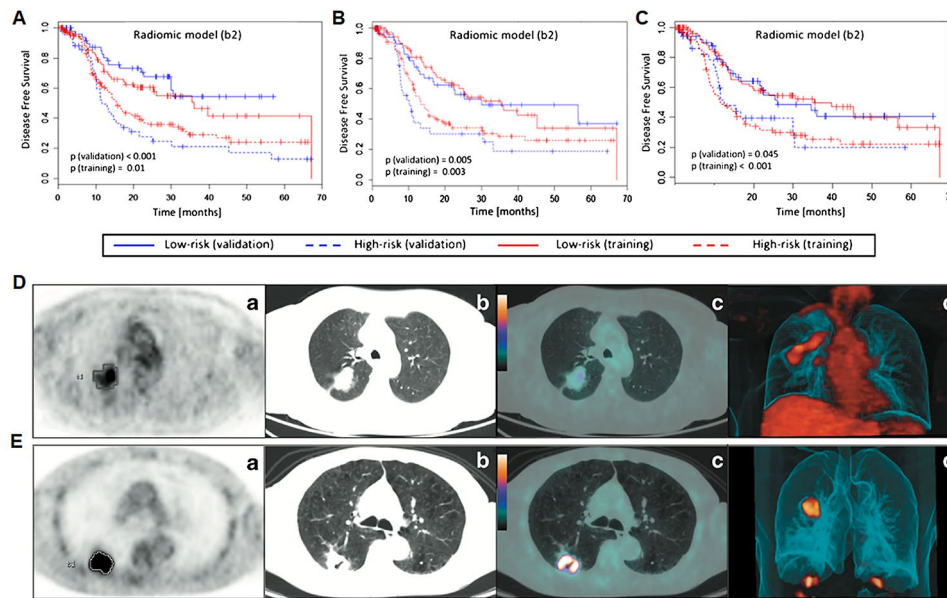
Fig. 3 PET/CT radiomics models for predicting disease-free survival in NSCLC patients undergoing surgery. Kaplan-Meier curves for the DFS resulting from the Cox regression models built using the radiomic signature within the CT (**A**), the PET (**B**) and the PET + CT (**C**) dataset. The AUCs for the different Cox regression models were 0.75 (95% CI:0.65–0.85), 0.68 (95%CI: 0.57–0.80) and 0.68 (95%CI: 0.58–0.74). Clinical cases PET/CT images of a low-risk (**D**) and a high-risk (**E**) patient. Low-risk patient: axial PET, CT, PET/CT and a three-dimensional reconstruction of PET/CT images (**a**, **b**, **c**, and **d**, respectively) of a 64-year-old female with ADC, pathological stage 2a (T2N0M0), with no evidence of disease 31 months after surgery. High-risk patient: axial PET, CT, PET/CT, and a three-dimensional reconstruction of PET/CT images (**a**, **b**, **c** and **d**, respectively) of a 60-year-old male, with squamous cell carcinoma, pathological stage 2a (T2N0M0), who experienced disease recurrence 11 months after surgery. Data derived from Kirienko et al. [150]

Different ML algorithms will yield models with varying performances in outcome stratification of patients [156]. Sepehri et al. [156] prospectively conducted an assessment of the effectiveness of a ^{18}F-FDG PET/CT-based radiomics model built using the consensus of 3 ML algorithms for the prediction of outcomes in patients with stage II-III NSCLC. Three different ML pipelines (SVM, random forest, and LR) were exploited to predictively classify OS into binary groups. Two clinical endpoints, namely the median OS and OS less than 6 months, were examined. The results highlighted that distinct ML methods demonstrate huge differences in feature selection and achieved differing levels of classification performance and as well demonstrated that a collective agreement of ML algorithms could enhance the radiomics performance. In both scenarios, averaging probabilities improved the results better than majority voting. While additional validation of these preliminary findings in a larger sample size cohort is necessary, the present study holds promise for pinpoint higher-risk cases within stage II-III populations, thereby allowing for the implementation of more intensive interventions and increased frequency of post-treatment follow-ups, which could result in significant benefits for those individuals.

Challenges and future direction

Radiomics in NMI possesses the potential to extract archetypal signatures as substitute biomarkers to identify cancer characteristics, which is attributed to the ability to capture tumor heterogeneity non-invasively and to show anatomical and functional information simultaneously, and it has seen significant progress over the past decade in this field.

Despite the rapid growth, the focus of radiomics research remains predominantly on the proof of concept stage and the transformation from a top-tier research area into an indispensable clinical decision-making strategy is in high demand [23]. To achieve this, there exist obstacles that are imperative to be tackled before it can be effectively incorporated into clinical practice.

The robustness and reproducibility of radiomics factors are subject to variability due to diverse factors including the image acquisition protocols (e.g. patient preparation, radiotracer dosage and uptake time), scanner vendors, reconstruction algorithms (e.g. matching of resolution and iterative reconstruction convergence) and data analysis [157, 158]. The inferior spatial resolution and unsatisfactory statistical attributes of PET images can engender greater instability [159]. To improve the generalization of radiomics researches, it is necessary to establish inter-institutional standardized imaging parameters, reconstruction technologies and segmentation methods, that will facilitate the successful application of promising outcomes that are found in one particular study to be utilized in another [160]. PET imaging guidelines, including those proposed by EANM [21] and a Netherlands cooperative group [161], can provide unified specifications in multi-center PET studies and it's the responsibility of manufacturers and researchers to support the implementation and maintenance of these guidelines in future studies and practice. Additionally, considerable disparity exists between the definitions and nomenclature of features in current literature and available software [162]. The Quantitative Imaging Biomarkers Alliance (QIBA) [163] and IBSI [55] are being undertaken to facilitate the harmonization of the definitions, reference values and calculation schemes of quantitative imaging biomarkers, enhancing the reproducibility and comparability. Post-harmonization techniques such as ComBat are proposed to address the batch effect variability, improve model performance and increase data sharing capabilities. However, there are concerns that these techniques may notably alter feature values and even result in impossible values, e.g. negative volume values, for which further in-depth investigation is needed [23, 164].

As previously discussed, validation of the established model is a crucial component in radiomics pipeline. The TRIPOD (i.e. transparent reporting of a multivariable prediction model for individual prognosis or diagnosis) statement highlights that development of prediction models should always include validation to quantify overestimation or bias in the predictive performance [165]. The absence of multi-center studies and external validation in existing literature decreases the reliability of positive outcomes and presents a limitation to the clinical translation of radiomics [166, 167]. For further studies, it is necessary to employ large, multi-center cohorts in model validation to mitigate the risk of statistical biases and avoid over-positive findings [162]. One concerns the creation of large, publicly available, open access image databases, which preferably should be encouraged by public organisations.

For past published papers, uniform assessment criteria are needed to incorporate a publication into confound meta-analyses and reviews. Lambin et al. [7] proposed a radiomics quality score (RQS) for evaluating the quality of radiomics researches and promoting the execution of standardized guidelines and rigorous reporting requirements. It consists of 16 items such as the image protocol compliance and reporting, multiple segmentations, imaging at multiple time points, multivariable analysis with non-radiomics features, validation and cost-effectiveness analysis. RQS can enable researchers to ensure

the high-quality of their studies that are likely to generate meaningful outcomes, as well as assist readers in identifying the reliability and informativeness [168]. Despite its usefulness, however, the RQS score has limitations that some components are not universally applicable, while some have relatively ambiguous score criteria and additionally, inter-reviewer discrepancies exist [169]. It is important to acknowledge these limitations and use the RQS in conjunction with other methods to get a more accurate and complete picture of the quality of a study [170]. Adhering more closely to established guidelines is essential for facilitating the widespread adoption of radiomics and machine learning in routine clinical practice [171].

Although radiomics studies have garnered increasing interest in recent years, their integration into large-scale clinical trials has been relatively slow. Despite radiomics approaches potentially offering the highest level of evidence, only a few trials have included radiomics projects as ancillary studies. Incorporating radiomics approaches into large clinical trials could catalyze the rapid development of radiomics, accelerating the translation of scientific theories from preclinical experimentation to clinical implementation, ultimately conferring benefits to more patients. There is a pressing need for collaborative efforts between radiologists, oncologists, and biostatisticians to propel the integration.

Artificial intelligence (AI) technologies including classical ML and DL have penetrated into various procedures of radiomics including but not limited to image reconstruction, segmentation, extraction of radiomics features and data analysis and opened up new possibilities for NMI, paving the way for more effective and personalized patient care [172]. One of the factors hindering the wider application of AI in clinical practice is its tendency to sacrifice interpretability in favor of better prediction accuracy, resulting in the so-called "black box" problem [173]. Graph-based methods and advanced visualization tools represent as promising approaches to enhance the interpretability of radiomics data for clinicians [173].

As for lung cancer, it is suggested that in future studies, radiomics may need to be combined with more clinical risk factors for instance the patient's performance status, smoking habits and complications including pneumonia and chronic obstructive pulmonary disease in order to accurately predict survival of lung cancer patients [23, 174]. Compared to CT, PET studies on the correlation between RFs and tumor biology, such as gene expression or blood serum biomarkers, are less in number and yield less satisfactory outcomes [23]. To advance PET radiomics studies in lung cancer, exploring multimodality studies in large patient cohorts and developing novel radiotracers that target other biomarkers and pathophysiological processes could be promising directions for future research. Furthermore, current radiomics researches are predominantly centered on NSCLC, while investigations into SCLC remain scarce. This paucity highlights the need for future endeavors to carry out studies focusing on SCLC to improve clinical management strategies.

Implementing AI in clinical practice presents challenges such as limited resources and the need for proper training and education among healthcare professionals. Healthcare systems should establish substantial infrastructure and training programs for all personnel to effectively use and interpret AI tools. In the context of rapidly evolving healthcare systems and workflows, these tools must be regularly updated to ensure seamless performance [175]. Additionally, maintaining patient privacy, data security, data ownership,

and compliance with regulations like HIPAA presents complexities. A framework with clear guidelines for the acceptance and deployment of AI models in healthcare is essential to guarantee patient safety and uphold ethical standards in data management.

Conclusion

In this review, we presented an outline of the radiomics workflow, its current progress in the context of lung cancer, the existing pitfalls and future directions. Overall, both nuclear medicine radiomics and its application in lung cancer are rapidly evolving fields that hold great promise for improving the accuracy of diagnosis, staging, and prognosis of lung cancer. Its ability to capture and analyze high-throughput quantitative imaging features directly related to the biological function provides valuable insights into tumor heterogeneity and can improve personalization of treatment plans. While there are still challenges to the implementation of PET radiomics in clinical practice, ongoing research efforts are addressing these challenges and it will play an increasingly important role in the management of lung cancer in the future.

Abbreviations

^{18}F-FDG	2-Deoxy-2-[fluorine-18]-fluoro-D-glucose
AD	Alzheimer's Disease
ADC	Adenocarcinoma
AI	Artificial intelligence
AUC	Area under the curve
C-index	Concordance index
CNN	Convolutional neural network
CPH	Cox proportional hazard
CT	Computed tomography
DFS	Disease-free survival
DL	Deep-learning
E19del	Exon 19 deletion
EANM	European Association of Nuclear Medicine
EARL	European Association of Nuclear Medicine Research Ltd
EFS	Evidential Feature Selection
EGFR	Epidermal growth factor receptor
FCN	Fully convolutional network
FSL	Few-shot learning
GTV	Gross tumor volume
IBSI	Image biomarker standardization initiative
ICC	Intraclass correlation coefficient
IoU	Intersection over union
kNN	k-nearest neighbors
LN	Lymph node
LR	Logistic regression
LVI	Lymphovascular invasion
MCI	Mild Cognitive Impairment
MDS	Multi-dimensional scaling
MICCAI	The Medical Image Computing and Computer Assisted Intervention
ML	Machine learning
MRI	Magnetic resonance imaging
MT	Mutant type
MTV	Metabolic tumor volume
NMI	Nuclear medicine imaging
NSCLC	Non-small cell lung cancer
OS	Overall survival
PCA	Principal component analysis
pCR	Pathological complete response
PET	Positron emission tomography
PFS	Progression-free survival
QIBA	Quantitative Imaging Biomarkers Alliance
RF	Radiomics feature
RFS	Recurrence-free survival
RQS	Radiomics quality score
ROI	Region of interest
SBRT	Stereotactic body radiotherapy
SCC	Squamous cell carcinoma

SPECT	Single photon emission computed tomography
SPN	Solitary pulmonary nodule
SSL	Semi-supervised learning
SUV	Standardized uptake value
SVM	Support vector machines
t-SNE	t-distributed stochastic neighbor embedding
TKI	Tyrosine kinase inhibitors
TLG	Total lesion glycolysis
TRIPOD	Transparent reporting of a multivariable prediction model for individual prognosis or diagnosis
VOI	Volume of interest
WT	Wild type

Data availability
The original contributions presented in the study are included in the article. Further inquiries can be directed to the corresponding author.

Declarations

Ethics approval and consent to participate
Not applicable.

Consent for publication
Not applicable.

Conflict of interest
All authors declare no conflict of interest.

References

1. Chen P, Liu Y, Wen Y, Zhou C. Non-small cell lung cancer in China. Cancer Commun (Lond). 2022;42(10):937–70.
2. Siegel RL, Miller KD, Fuchs HE, Jemal A. Cancer statistics, 2022. CA Cancer J Clin. 2022;72(1):7–33.
3. Torre LA, Siegel RL, Jemal A. Lung Cancer statistics. Adv Exp Med Biol. 2016;893:1–19.
4. Bade BC, Dela Cruz CS. Lung Cancer. 2020: Epidemiology, Etiology, and Prevention. Clin Chest Med. 2020;41(1):1–24.
5. Ettinger DS, Wood DE, Aisner DL, Akerley W, Bauman JR, Bharat A, et al. Non-small Cell Lung Cancer, Version 3.2022, NCCN Clinical Practice guidelines in Oncology. J Natl Compr Canc Netw. 2022;20(5):497–530.
6. Hood L, Friend SH. Predictive, personalized, preventive, participatory (P4) cancer medicine. Nat Rev Clin Oncol. 2011;8(3):184–7.
7. Lambin P, Leijenaar RTH, Deist TM, Peerlings J, de Jong EEC, van Timmeren J, et al. Radiomics: the bridge between medical imaging and personalized medicine. Nat Rev Clin Oncol. 2017;14(12):749–62.
8. Ge J, Zhang Q, Zeng J, Gu Z, Gao M. Radiolabeling nanomaterials for multimodality imaging: new insights into nuclear medicine and cancer diagnosis. Biomaterials. 2020;228:119553.
9. Beuthien-Baumann B, Sachpekidis C, Gnirs R, Sedlaczek O. Adapting imaging protocols for PET-CT and PET-MRI for Immunotherapy Monitoring. Cancers (Basel). 2021;13:23.
10. Kang F, Wang S, Tian F, Zhao M, Zhang M, Wang Z, et al. Comparing the diagnostic potential of 68Ga-Alfatide II and 18F-FDG in differentiating between Non-small Cell Lung Cancer and Tuberculosis. J Nucl Med. 2016;57(5):672–7.
11. Dingemans AC, Früh M, Ardizzoni A, Besse B, Faivre-Finn C, Hendriks LE, et al. Small-cell lung cancer: ESMO Clinical Practice guidelines for diagnosis, treatment and follow-up(☆). Ann Oncol. 2021;32(7):839–53.
12. Kostakoglu L, Chauvie S. PET-Derived quantitative Metrics for response and prognosis in Lymphoma. PET Clin. 2019;14(3):317–329.
13. Yildiz H, D'Abadie P, Gheysens O. The role of quantitative and semi-quantitative [F-18]FDG-PET/CT indices for evaluating Disease activity and management of patients with Dermatomyositis and Polymyositis. Volume 9. FRONTIERS IN MEDICINE; 2022.
14. Lambin P, Rios-Velazquez E, Leijenaar R, Carvalho S, van Stiphout R, Granton P, et al. Radiomics: extracting more information from medical images using advanced feature analysis. Eur J Cancer. 2012;48(4):441–6.
15. Conti A, Duggento A, Indovina I, Guerrisi M, Toschi N. Radiomics in breast cancer classification and prediction. Sem Cancer Biol. 2021;72:238–50.

16. Sollini M, Antunovic L, Chiti A, Kirienko M. Towards clinical application of image mining: a systematic review on artificial intelligence and radiomics. Volume 46. EUROPEAN JOURNAL OF NUCLEAR MEDICINE AND MOLECULAR IMAGING; 2019. pp. 2656–72. 13.

17. Limkin EJ, Sun R, Dercle L, Zacharaki EI, Robert C, Reuze S, et al. Promises and challenges for the implementation of computational medical imaging (radiomics) in oncology. Ann Oncol. 2017;28(6):1191–206.

18. Shiri I, Rahmim A, Ghaffarian P, Geramifar P, Abdollahi H, Bitarafan-Rajabi A. The impact of image reconstruction settings on 18F-FDG PET radiomic features: multi-scanner phantom and patient studies. Eur Radiol. 2017;27(11):4498–509.

19. Luo H, Zhuang Q, Wang Y, Abudumijiti A, Shi K, Rominger A, et al. A novel image signature-based radiomics method to achieve precise diagnosis and prognostic stratification of gliomas. Lab Invest. 2021;101(4):450–62.

20. Orlhac F, Eertink JJ, Cottereau AS, Zijlstra JM, Thieblemont C, Meignan M, et al. A guide to ComBat harmonization of imaging biomarkers in Multicenter studies. J Nucl Med. 2022;63(2):172–9.

21. Boellaard R, Delgado-Bolton R, Oyen WJ, Giammarile F, Tatsch K, Eschner W, et al. FDG PET/CT: EANM procedure guidelines for tumour imaging: version 2.0. Eur J Nucl Med Mol Imaging. 2015;42(2):328–54.

22. Aide N, Lasnon C, Veit-Haibach P, Sera T, Sattler B, Boellaard R. EANM/EARL harmonization strategies in PET quantification: from daily practice to multicentre oncological studies. Eur J Nucl Med Mol Imaging. 2017;44(Suppl 1):17–31.

23. Bogowicz M, Vuong D, Huellner MW, Pavic M, Andratschke N, Gabrys HS, et al. CT radiomics and PET radiomics: ready for clinical implementation? Q J Nuclear Med Mol Imaging. 2019;63(4):355–70.

24. Altazi BA, Zhang GG, Fernandez DC, Montejo ME, Hunt D, Werner J, et al. Reproducibility of F18-FDG PET radiomic features for different cervical tumor segmentation methods, gray-level discretization, and reconstruction algorithms. J Appl Clin Med Phys. 2017;18(6):32–48.

25. Pfaehler E, van Sluis J, Merema BBJ, van Ooijen P, Berendsen RCM, van Velden FHP, et al. Experimental multicenter and multivendor evaluation of the performance of PET radiomic features using 3-Dimensionally printed Phantom inserts. J Nucl Med. 2020;61(3):469–76.

26. Weisman AJ, Bradshaw TJ, Namias M, Jeraj R. Impact of scanner harmonization on PET-based treatment response assessment in metastatic melanoma. Phys Med Biol. 2020;65(22).

27. Johnson WE, Li C, Rabinovic A. Adjusting batch effects in microarray expression data using empirical Bayes methods. Biostatistics. 2007;8(1):118–27.

28. Orlhac F, Boughdad S, Philippe C, Stalla-Bourdillon H, Nioche C, Champion L, et al. A postreconstruction harmonization method for Multicenter Radiomic studies in PET. J Nucl Med. 2018;59(8):1321–8.

29. Mahon RN, Ghita M, Hugo GD, Weiss E. ComBat harmonization for radiomic features in independent phantom and lung cancer patient computed tomography datasets. Phys Med Biol. 2020;65(1):015010.

30. Leithner D, Schoder H, Haug A, Vargas HA, Gibbs P, Haggstrom I, et al. Impact of ComBat Harmonization on PET Radiomics-based tissue classification: a dual-center PET/MRI and PET/CT study. J Nucl Med. 2022;63(10):1611–6.

31. Chen WJ, Rae WID, Kench PL, Meikle SR. The potential advantages and workflow challenges of long axial field of view PET/CT. J Med Radiat Sci. 2023;70(3):310–8.

32. Schillaci O, Urbano N. Digital PET/CT: a new intriguing chance for clinical nuclear medicine and personalized molecular imaging. Eur J Nucl Med Mol Imaging. 2019;46(6):1222–5.

33. Liu RJ, Elhalawani H, Mohamed ASR, Elgohari B, Court L, Zhu HT, et al. Stability analysis of CT radiomic features with respect to segmentation variation in oropharyngeal cancer. Clin Translational Radiation Oncol. 2020;21:11–8.

34. Gallivanone F, Interlenghi M, D'Ambrosio D, Trifiro G, Castiglioni I. Parameters influencing PET imaging features: a Phantom study with irregular and heterogeneous synthetic lesions. Contrast Media & Molecular Imaging; 2018.

35. Kolinger GD, Vállez García D, Kramer GM, Frings V, Smit EF, de Langen AJ, et al. Repeatability of [(18)F]FDG PET/CT total metabolic active tumour volume and total tumour burden in NSCLC patients. EJNMMI Res. 2019;9(1):14.

36. Yip SSF, Aerts H. Applications and limitations of radiomics. Phys Med Biol. 2016;61(13):R150–66.

37. Parmar C, Velazquez ER, Leijenaar R, Jermoumi M, Carvalho S, Mak RH et al. Robust Radiomics feature quantification using semiautomatic volumetric segmentation. PLoS ONE. 2014;9(7).

38. Zhang XP, Zhang YC, Zhang GJ, Qiu XT, Tan WJ, Yin XX et al. Deep learning with Radiomics for Disease diagnosis and treatment: challenges and potential. Front Oncol. 2022;12.

39. Tsai MH, Wang MH, Chang TY, Pai PY, Chan YK, editors. An Adaptable Threshold Decision Method. 2009 Fifth International Conference on Information Assurance and Security; 2009 18–20 Aug. 2009.

40. Zaidi H, El Naqa I. PET-guided delineation of radiation therapy treatment volumes: a survey of image segmentation techniques. Eur J Nucl Med Mol Imaging. 2010;37(11):2165–87.

41. Foster B, Bagci U, Mansoor A, Xu ZY, Mollura DJ. A review on segmentation of positron emission tomography images. Comput Biol Med. 2014;50:76–96.

42. Ferrante M, Rinaldi L, Botta F, Hu X, Dolp A, Minotti M, et al. Application of nnu-net for automatic segmentation of lung lesions on CT images and its implication for Radiomic models. J Clin Med. 2022;11:24.

43. Hesamian MH, Jia W, He XJ, Kennedy P. Deep learning techniques for Medical Image Segmentation: achievements and challenges. J Digit Imaging. 2019;32(4):582–96.

44. Pfaehler E, Mesotten L, Kramer G, Thomeer M, Vanhove K, de Jong J et al. Repeatability of two semi-automatic artificial intelligence approaches for tumor segmentation in PET. Ejnmmi Res. 2021;11(1).

45. Hatt M, Laurent B, Ouahabi A, Fayad H, Tan S, Li L, et al. The first MICCAI challenge on PET tumor segmentation. Med Image Anal. 2018;44:177–95.

46. Ronneberger O, Fischer P, Brox T, editors. U-Net: Convolutional Networks for Biomedical Image Segmentation. Medical Image Computing and Computer-assisted intervention – MICCAI 2015; 2015 2015//; Cham: Springer International Publishing.

47. Alom MZ, Yakopcic C, Hasan M, Taha TM, Asari VK. Recurrent residual U-Net for medical image segmentation. J Med Imaging. 2019;6(1).

48. Wang HL, Wang ZH, Wang JL, Li K, Geng GH, Kang F et al. ICA-Unet: an improved U-net network for brown adipose tissue segmentation. J Innovative Opt Health Sci. 2022;15(03).

49. Spuhler K, Serrano-Sosa M, Cattell R, DeLorenzo C, Huang C. Full-count PET recovery from low-count image using a dilated convolutional neural network. Med Phys. 2020;47(10):4928–38.

50. Milletari F, Navab N, Ahmadi S-A, editors. V-net: Fully convolutional neural networks for volumetric medical image segmentation. 2016 fourth international conference on 3D vision (3DV); 2016: Ieee.

51. Li LQ, Zhao XM, Lu W, Tan S. Deep learning for variational multimodality tumor segmentation in PET/CT. Neurocomputing. 2020;392:277–95.

52. Protonotarios NE, Katsamenis I, Sykiotis S, Dikaios N, Kastis GA, Chatziioannou SN et al. A few-shot U-Net deep learning model for lung cancer lesion segmentation via PET/CT imaging. Biomedical Phys Eng Express. 2022;8(2).

53. Mayerhoefer ME, Materka A, Langs G, Häggström I, Szczypiński P, Gibbs P, et al. Introduction to Radiomics. J Nucl Med. 2020;61(4):488–95.

54. Zwanenburg A, Leger S, Vallières M, Löck S. Image biomarker standardisation initiative-feature definitions. arXiv preprint arXiv:161207003. 2016;10.

55. Zwanenburg A, Vallieres M, Abdalah MA, Aerts H, Andrearczyk V, Apte A, et al. The image Biomarker Standardization Initiative: standardized quantitative Radiomics for High-Throughput Image-based phenotyping. Radiology. 2020;295(2):328–38.

56. Apte AP, Iyer A, Crispin-Ortuzar M, Pandya R, van Dijk LV, Spezi E et al. Technical note: extension of CERR for computational radiomics: a comprehensive MATLAB platform for reproducible radiomics research. Med Phys. 2018.

57. Fedorov A, Beichel R, Kalpathy-Cramer J, Finet J, Fillion-Robin JC, Pujol S, et al. 3D slicer as an image computing platform for the quantitative Imaging Network. Magn Reson Imaging. 2012;30(9):1323–41.

58. van Griethuysen JJM, Fedorov A, Parmar C, Hosny A, Aucoin N, Narayan V, et al. Computational Radiomics System to Decode the Radiographic phenotype. Cancer Res. 2017;77(21):e104–7.

59. Nioche C, Orlhac F, Boughdad S, Reuzé S, Goya-Outi J, Robert C, et al. LIFEx: a freeware for Radiomic feature calculation in Multimodality Imaging to accelerate advances in the characterization of Tumor Heterogeneity. Cancer Res. 2018;78(16):4786–9.

60. Pfaehler E, Zwanenburg A, de Jong JR, Boellaard R. RaCaT: an open source and easy to use radiomics calculator tool. PLoS ONE. 2019;14(2):e0212223.

61. Fang YH, Lin CY, Shih MJ, Wang HM, Ho TY, Liao CT, et al. Development and evaluation of an open-source software package CGITA for quantifying tumor heterogeneity with molecular images. Biomed Res Int. 2014;2014:248505.

62. Zinsz A, Pouget C, Rech F, Taillandier L, Blonski M, Amlal S et al. The role of 18 F FDOPA PET as an adjunct to conventional MRI in the diagnosis of aggressive glial lesions. Eur J Nucl Med Mol Imaging. 2024.

63. Voltin CA, Paccagnella A, Winkelmann M, Heger JM, Casadei B, Beckmann L, et al. Multicenter development of a PET-based risk assessment tool for product-specific outcome prediction in large B-cell lymphoma patients undergoing CAR T-cell therapy. Eur J Nucl Med Mol Imaging. 2024;51(5):1361–70.

64. Fornacon-Wood I, Mistry H, Ackermann CJ, Blackhall F, McPartlin A, Faivre-Finn C, et al. Reliability and prognostic value of radiomic features are highly dependent on choice of feature extraction platform. Eur Radiol. 2020;30(11):6241–50.

65. Foy JJ, Robinson KR, Li H, Giger ML, Al-Hallaq H, Armato SG. 3rd. Variation in algorithm implementation across radiomics software. J Med Imaging (Bellingham). 2018;5(4):044505.

66. Jia WK, Sun ML, Lian J, Hou SJ. Feature dimensionality reduction: a review. Complex Intell Syst. 2022;8(3):2663–93.

67. Parekh V, Jacobs MA. Radiomics: a new application from established techniques. Expert Rev Precis Med Drug Dev. 2016;1(2):207–26.

68. Nasteski V. An overview of the supervised machine learning methods. Horizons b. 2017;4:51–62.

69. Jolliffe IT, Cadima J. Principal component analysis: a review and recent developments. Philosophical Transactions of the Royal Society a-Mathematical Physical and Engineering Sciences. 2016;374(2065).

70. Van der Maaten L, Hinton G. Visualizing data using t-SNE. J Mach Learn Res. 2008;9(11).

71. Bengio Y, Paiement JFO, Vincent P, Delalleau O, Le Roux N, Ouimet M, editors. Out-of-sample extensions for LLE, isomap, MDS, eigenmaps, and spectral clustering. 17th Annual Conference on Neural Information Processing Systems (NIPS); 2003; Canada2004.

72. Lin P, Lin YQ, Gao RZ, Wen R, Qin H, He Y et al. Radiomic profiling of clear cell renal cell carcinoma reveals subtypes with distinct prognoses and molecular pathways. Translational Oncol. 2021;14(7).

73. Anowar F, Sadaoui S, Selim B. Conceptual and empirical comparison of dimensionality reduction algorithms (PCA, KPCA, LDA, MDS, SVD, LLE, ISOMAP, LE, ICA, t-SNE). Comput Sci Rev. 2021;40:100378.

74. Lian C, Ruan S, Denœux T, Jardin F, Vera P. Selecting radiomic features from FDG-PET images for cancer treatment outcome prediction. Med Image Anal. 2016;32:257–68.

75. Shafiq-Ul-Hassan M, Latifi K, Zhang G, Ullah G, Gillies R, Moros E. Voxel size and gray level normalization of CT radiomic features in lung cancer. Sci Rep. 2018;8(1):10545.

76. Depeursinge A, Foncubierta-Rodriguez A, Van De Ville D, Müller H. Three-dimensional solid texture analysis in biomedical imaging: review and opportunities. Med Image Anal. 2014;18(1):176–96.

77. Whybra P, Parkinson C, Foley K, Staffurth J, Spezi E. Assessing radiomic feature robustness to interpolation in F-18-FDG PET imaging. Sci Rep. 2019;9.

78. Liu JF, Guo W, Zeng PE, Geng YY, Liu Y, Ouyang HQ, et al. Vertebral MRI-based radiomics model to differentiate multiple myeloma from metastases: influence of features number on logistic regression model performance. Eur Radiol. 2022;32(1):572–81.

79. Li MM, Wang HF, Shang ZG, Yang ZL, Zhang Y, Wan H. Ependymoma and pilocytic astrocytoma: differentiation using radiomics approach based on machine learning. J Clin Neurosci. 2020;78:175–80.

80. Yun J, Park JE, Lee H, Ham S, Kim N, Kim HS. Radiomic features and multilayer perceptron network classifier: a robust MRI classification strategy for distinguishing glioblastoma from primary central nervous system lymphoma. Sci Rep. 2019;9(1):5746.

81. Haubold J, Demircioglu A, Gratz M, Glas M, Wrede K, Sure U, et al. Non-invasive tumor decoding and phenotyping of cerebral gliomas utilizing multiparametric (18)F-FET PET-MRI and MR Fingerprinting. Eur J Nucl Med Mol Imaging. 2020;47(6):1435–45.

82. Shang SJ, Sun J, Yue ZB, Wang YN, Wang XY, Luo YH et al. Multi-parametric MRI based radiomics with tumor subregion partitioning for differentiating benign and malignant soft-tissue tumors. Biomed Signal Process Control. 2021;67.

83. Choi YS, Bae S, Chang JH, Kang SG, Kim SH, Kim J, et al. Fully automated hybrid approach to predict the IDH mutation status of gliomas via deep learning and radiomics. Neurooncology. 2021;23(2):304–13.

84.   Torresan F, Crimi F, Ceccato F, Zavan F, Barbot M, Lacognata C et al. Radiomics: a new tool to differentiate adrenocortical adenoma from carcinoma. Bjs Open. 2021;5(1).

85.   Wang DQ, Zhang X, Liu H, Qiu B, Liu SR, Zheng CJ, et al. Assessing dynamic metabolic heterogeneity in non-small cell lung cancer patients via ultra-high sensitivity total-body F-18 FDG PET/CT imaging: quantitative analysis of F-18 FDG uptake in primary tumors and metastatic lymph nodes. Eur J Nucl Med Mol Imaging. 2022;49(13):4692–704.

86.   Lin P, Peng YT, Gao RZ, Wei Y, Li XJ, Huang SN, et al. Radiomic profiles in diffuse glioma reveal distinct subtypes with prognostic value. J Cancer Res Clin Oncol. 2020;146(5):1253–62.

87.   Zhu Y, Tan Y, Hua Y, Wang M, Zhang G, Zhang J. Feature selection and performance evaluation of support vector machine (SVM)-based classifier for differentiating benign and malignant pulmonary nodules by computed tomography. J Digit Imaging. 2010;23(1):51–65.

88.   Wu Y, Jiang JH, Chen L, Lu JY, Ge JJ, Liu FT et al. Use of radiomic features and support vector machine to distinguish Parkinson's disease cases from normal controls. Annals Translational Med. 2019;7(23).

89.   Choi W, Liu CJ, Alam SR, Oh JH, Vaghjiani R, Humm J, et al. Preoperative (18)F-FDG PET/CT and CT radiomics for identifying aggressive histopathological subtypes in early stage lung adenocarcinoma. Comput Struct Biotechnol J. 2023;21:5601–8.

90.   Avanzo M, Stancanello J, El Naqa I. Beyond imaging: the promise of radiomics. Phys Medica-European J Med Phys. 2017;38:122–39.

91.   Janghel RR, Rathore YK. Deep convolution neural network based system for early diagnosis of Alzheimer's Disease. Irbm. 2021;42(4):258–67.

92.   Zhu J, Shi J, Liu X, Chen X, Ieee, editors. Co-Training Based Semi-supervised Classification of Alzheimer's Disease. 19th International Conference on Digital Signal Processing (DSP); 2014 Aug 20–23; Hong Kong, PEOPLES R CHINA2014.

93.   Solatidehkordi Z, Zualkernan I. Survey on recent trends in medical image classification using Semi-supervised Learning. Appl Sciences-Basel. 2022;12(23).

94.   Lu S, Xia Y, Cai WD, Fulham M, Feng DD, Alzheimer's Dis N. Early identification of mild cognitive impairment using incomplete random forest-robust support vector machine and FDG-PET imaging. Comput Med Imaging Graph. 2017;60:35–41.

95.   Moons KG, Altman DG, Reitsma JB, Ioannidis JP, Macaskill P, Steyerberg EW, et al. Transparent reporting of a multivariable prediction model for individual prognosis or diagnosis (TRIPOD): explanation and elaboration. Ann Intern Med. 2015;162(1):W1–73.

96.   Wesdorp NJ, Hellingman T, Jansma EP, van Waesberghe J, Boellaard R, Punt CJA, et al. Advanced analytics and artificial intelligence in gastrointestinal cancer: a systematic review of radiomics predicting response to treatment. Eur J Nucl Med Mol Imaging. 2021;48(6):1785–94.

97.   Wang XL, Shan W. Application of dynamic CT to identify lung cancer, pulmonary tuberculosis, and pulmonary inflammatory pseudotumor. Eur Rev Med Pharmacol Sci. 2017;21(21):4804–9.

98.   Hu Y, Zhao X, Zhang J, Han J, Dai M. Value of (18)F-FDG PET/CT radiomic features to distinguish solitary lung adenocarcinoma from tuberculosis. Eur J Nucl Med Mol Imaging. 2021;48(1):231–40.

99.   Zhang X, Dong X, Saripan MIB, Du D, Wu Y, Wang Z, et al. Deep learning PET/CT-based radiomics integrates clinical data: a feasibility study to distinguish between Tuberculosis nodules and lung cancer. Thorac Cancer. 2023;14(19):1802–11.

100. Zhang Y, Liu H, Chang C, Yin Y, Wang R. Machine learning for differentiating lung squamous cell cancer from adenocarcinoma using clinical-metabolic characteristics and 18F-FDG PET/CT radiomics. PLoS ONE. 2024;19(4):e0300170.

101. Bashir U, Kawa B, Siddique M, Mak SM, Nair A, McLean E, et al. Non-invasive classification of non-small cell lung cancer: a comparison between random forest models utilising radiomic and semantic features. Br J Radiol. 2019;92(1099):20190159.

102. Dong X, Sun X, Sun L, Maxim PG, Xing L, Huang Y, et al. Early change in metabolic tumor heterogeneity during Chemoradiotherapy and its prognostic value for patients with locally Advanced Non-small Cell Lung Cancer. PLoS ONE. 2016;11(6):e0157836.

103. Ji Y, Qiu Q, Fu J, Cui K, Chen X, Xing L, et al. Stage-specific PET Radiomic Prediction Model for the histological subtype classification of Non-small-cell Lung Cancer. Cancer Manag Res. 2021;13:307–17.

104. Zheng J, Hao Y, Guo Y, Du M, Wang P, Xin J. An 18F-FDG-PET/CT-based radiomics signature for estimating malignance probability of solitary pulmonary nodule. Clin Respir J. 2024;18(5):e13751.

105. Salihoğlu YS, Uslu Erdemir R, Aydur Püren B, Özdemir S, Uyulan Ç, Ergüzel TT, et al. Diagnostic performance of machine learning models based on (18)F-FDG PET/CT Radiomic features in the classification of Solitary Pulmonary nodules. Mol Imaging Radionucl Ther. 2022;31(2):82–8.

106. Sung SY, Kwak YK, Lee SW, Jo IY, Park JK, Kim KS, et al. Lymphovascular Invasion increases the risk of Nodal and distant recurrence in node-negative stage I-IIA non-small-cell Lung Cancer. Oncology. 2018;95(3):156–62.

107. Wang J, Zheng Z, Zhang Y, Tan W, Li J, Xing L, et al. (18)F-FDG PET/CT radiomics for prediction of lymphovascular invasion in patients with early stage non-small cell lung cancer. Front Oncol. 2023;13:1185808.

108. Zheng Z, Wang J, Tan W, Zhang Y, Li J, Song R, et al. (18)F-FDG PET/CT radiomics predicts brain metastasis in I-IIIA resected non-small cell lung cancer. Eur J Radiol. 2023;165:110933.

109. Okazaki T, Chikuma S, Iwai Y, Fagarasan S, Honjo T. A rheostat for immune responses: the unique properties of PD-1 and their advantages for clinical application. Nat Immunol. 2013;14(12):1212–8.

110. Chen Q, Zhang L, Mo X, You J, Chen L, Fang J, et al. Current status and quality of radiomic studies for predicting immunotherapy response and outcome in patients with non-small cell lung cancer: a systematic review and meta-analysis. Eur J Nucl Med Mol Imaging. 2021;49(1):345–60.

111. Jiang M, Sun D, Guo Y, Guo Y, Xiao J, Wang L, et al. Assessing PD-L1 expression level by Radiomic features from PET/CT in Nonsmall Cell Lung Cancer patients: an initial result. Acad Radiol. 2020;27(2):171–9.

112. Zhang R, Hohenforst-Schmidt W, Steppert C, Sziklavari Z, Schmidkonz C, Atzinger A, et al. Standardized 18F-FDG PET/CT radiomic features provide information on PD-L1 expression status in treatment-naïve patients with non-small cell lung cancer. Nuklearmedizin. 2022;61(5):385–93.

113. Li B, Su J, Liu K, Hu C. Deep learning radiomics model based on PET/CT predicts PD-L1 expression in non-small cell lung cancer. Eur J Radiol Open. 2024;12:100549.

114. Tang W, Li X, Xie X, Sun X, Liu J, Zhang J, et al. EGFR inhibitors as adjuvant therapy for resected non-small cell lung cancer harboring EGFR mutations. Lung Cancer. 2019;136:6–14.

115. Cheng H, Li XJ, Wang XJ, Chen ZW, Wang RQ, Zhong HC, et al. A meta-analysis of adjuvant EGFR-TKIs for patients with resected non-small cell lung cancer. Lung Cancer. 2019;137:7–13.

116. Leduc C, Merlio JP, Besse B, Blons H, Debieuvre D, Bringuier PP, et al. Clinical and molecular characteristics of non-small-cell lung cancer (NSCLC) harboring EGFR mutation: results of the nationwide French Cooperative Thoracic Intergroup (IFCT) program. Ann Oncol. 2017;28(11):2715–24.

117. Zhou Q, Zhang XC, Chen ZH, Yin XL, Yang JJ, Xu CR, et al. Relative abundance of EGFR mutations predicts benefit from gefitinib treatment for advanced non-small-cell lung cancer. J Clin Oncol. 2011;29(24):3316–21.

118. Lee CK, Davies L, Wu YL, Mitsudomi T, Inoue A, Rosell R et al. Gefitinib or Erlotinib vs Chemotherapy for EGFR mutation-positive Lung Cancer: Individual Patient Data Meta-Analysis of overall survival. J Natl Cancer Inst. 2017;109(6).

119. Sutiman N, Tan SW, Tan EH, Lim WT, Kanesvaran R, Ng QS, et al. EGFR Mutation subtypes Influence Survival outcomes following first-line gefitinib therapy in advanced Asian NSCLC patients. J Thorac Oncol. 2017;12(3):529–38.

120. Liu Q, Sun D, Li N, Kim J, Feng D, Huang G, et al. Predicting EGFR mutation subtypes in lung adenocarcinoma using (18)F-FDG PET/CT radiomic features. Transl Lung Cancer Res. 2020;9(3):549–62.

121. Li X, Yin G, Zhang Y, Dai D, Liu J, Chen P, et al. Predictive power of a Radiomic signature based on (18)F-FDG PET/CT images for EGFR Mutational Status in NSCLC. Front Oncol. 2019;9:1062.

122. Zhao HY, Su YX, Zhang LH, Fu P. Prediction model based on 18F-FDG PET/CT radiomic features and clinical factors of EGFR mutations in lung adenocarcinoma. Neoplasma. 2022;69(1):233–41.

123. Yang L, Xu P, Li M, Wang M, Peng M, Zhang Y, et al. PET/CT Radiomic features: a potential biomarker for EGFR Mutation Status and Survival Outcome Prediction in NSCLC patients treated with TKIs. Front Oncol. 2022;12:894323.

124. Yang B, Ji HS, Zhou CS, Dong H, Ma L, Ge YQ, et al. (18)F-fluorodeoxyglucose positron emission tomography/computed tomography-based radiomic features for prediction of epidermal growth factor receptor mutation status and prognosis in patients with lung adenocarcinoma. Transl Lung Cancer Res. 2020;9(3):563–74.

125. Abdurixiti M, Nijiati M, Shen R, Ya Q, Abuduxiku N, Nijiati M. Current progress and quality of radiomic studies for predicting EGFR mutation in patients with non-small cell lung cancer using PET/CT images: a systematic review. Br J Radiol. 2021;94(1122):20201272.

126. Chen J, Chen A, Yang S, Liu J, Xie C, Jiang H. Accuracy of machine learning in preoperative identification of genetic mutation status in lung cancer: a systematic review and meta-analysis. Radiother Oncol. 2024;196:110325.

127. Mok T, Ladrera G, Srimuninnimit V, Sriuranpong V, Yu CJ, Thongprasert S, et al. Tumor marker analyses from the phase III, placebo-controlled, FASTACT-2 study of intercalated erlotinib with gemcitabine/platinum in the first-line treatment of advanced non-small-cell lung cancer. Lung Cancer. 2016;98:1–8.

128. Wang J, Lv X, Huang W, Quan Z, Li G, Wu S, et al. Establishment and optimization of Radiomics algorithms for Prediction of KRAS Gene Mutation by Integration of NSCLC Gene Mutation Mutual Exclusion Information. Front Pharmacol. 2022;13:862581.

129. Bourbonne V, Morjani M, Pradier O, Hatt M, Jaouen V, Querellou S et al. PET/CT-Based Radiogenomics supports KEAP1/NFE2L2 pathway targeting for Non-small Cell Lung Cancer treated with curative Radiotherapy. J Nucl Med. 2024.

130. Muz B, de la Puente P, Azab F, Azab AK. The role of hypoxia in cancer progression, angiogenesis, metastasis, and resistance to therapy. Hypoxia (Auckl). 2015;3:83–92.

131. Xu Z, Li XF, Zou H, Sun X, Shen B. (18)F-Fluoromisonidazole in tumor hypoxia imaging. Oncotarget. 2017;8(55):94969–79.

132. Challapalli A, Carroll L, Aboagye EO. Molecular mechanisms of hypoxia in cancer. Clin Transl Imaging. 2017;5(3):225–53.

133. Zegers CM, van Elmpt W, Wierts R, Reymen B, Sharifi H, Öllers MC, et al. Hypoxia imaging with [18F]HX4 PET in NSCLC patients: defining optimal imaging parameters. Radiother Oncol. 2013;109(1):58–64.

134. Sanduleanu S, Jochems A, Upadhaya T, Even AJG, Leijenaar RTH, Dankers F, et al. Non-invasive imaging prediction of tumor hypoxia: a novel developed and externally validated CT and FDG-PET-based radiomic signatures. Radiother Oncol. 2020;153:97–105.

135. Devarakonda S, Morgensztern D, Govindan R. Genomic alterations in lung adenocarcinoma. Lancet Oncol. 2015;16(7):e342–51.

136. Siegel RL, Miller KD, Fuchs HE, Jemal A. Cancer statistics, 2021. CA Cancer J Clin. 2021;71(1):7–33.

137. Cuaron J, Dunphy M, Rimner A. Role of FDG-PET scans in staging, response assessment, and follow-up care for non-small cell lung cancer. Front Oncol. 2012;2:208.

138. Li J, Liu Y, Dong W, Zhou Y, Wu J, Luan K, et al. Identifying (18)F-FDG PET-metabolic radiomic signature for lung adenocarcinoma prognosis via the leveraging of prognostic transcriptomic module. Quant Imaging Med Surg. 2022;12(3):1893–908.

139. Chen YH, Wang TF, Chu SC, Lin CB, Wang LY, Lue KH, et al. Incorporating radiomic feature of pretreatment 18F-FDG PET improves survival stratification in patients with EGFR-mutated lung adenocarcinoma. PLoS ONE. 2020;15(12):e0244502.

140. Park SY, Cho A, Yu WS, Lee CY, Lee JG, Kim DJ, et al. Prognostic value of total lesion glycolysis by 18F-FDG PET/CT in surgically resected stage IA non-small cell lung cancer. J Nucl Med. 2015;56(1):45–9.

141. Yoo Ie R, Chung SK, Park HL, Choi WH, Kim YK, Lee KY, et al. Prognostic value of SUVmax and metabolic tumor volume on 18F-FDG PET/CT in early stage non-small cell lung cancer patients without LN metastasis. Biomed Mater Eng. 2014;24(6):3091–103.

142. Takeda A, Yokosuka N, Ohashi T, Kunieda E, Fujii H, Aoki Y, et al. The maximum standardized uptake value (SUVmax) on FDG-PET is a strong predictor of local recurrence for localized non-small-cell lung cancer after stereotactic body radiotherapy (SBRT). Radiother Oncol. 2011;101(2):291–7.

143. Provencio M, Nadal E, Insa A, García-Campelo MR, Casal-Rubio J, Dómine M, et al. Neoadjuvant chemotherapy and nivolumab in resectable non-small-cell lung cancer (NADIM): an open-label, multicentre, single-arm, phase 2 trial. Lancet Oncol. 2020;21(11):1413–22.

144. Yang M, Li X, Cai C, Liu C, Ma M, Qu W et al. [(18)F]FDG PET-CT radiomics signature to predict pathological complete response to neoadjuvant chemoimmunotherapy in non-small cell lung cancer: a multicenter study. Eur Radiol. 2023.

145. Schneider BJ, Daly ME, Kennedy EB, Antonoff MB, Broderick S, Feldman J, et al. Stereotactic body Radiotherapy for Early-Stage Non-small-cell Lung Cancer: American Society of Clinical Oncology Endorsement of the American Society for Radiation Oncology Evidence-Based Guideline. J Clin Oncol. 2018;36(7):710–9.

146. Nemoto H, Saito M, Satoh Y, Komiyama T, Marino K, Aoki S et al. Evaluation of the performance of both machine learning models using PET and CT radiomics for predicting recurrence following lung stereotactic body radiation therapy: a single-institutional study. J Appl Clin Med Phys. 2024:e14322.

147. Lucia F, Louis T, Cousin F, Bourbonne V, Visvikis D, Mievis C, et al. Multicentric development and evaluation of [(18)F]FDG PET/CT and CT radiomic models to predict regional and/or distant recurrence in early-stage non-small cell lung cancer treated by stereotactic body radiation therapy. Eur J Nucl Med Mol Imaging. 2024;51(4):1097–108.
148. Krarup MMK, Nygård L, Vogelius IR, Andersen FL, Cook G, Goh V, et al. Heterogeneity in tumours: validating the use of radiomic features on (18)F-FDG PET/CT scans of lung cancer patients as a prognostic tool. Radiother Oncol. 2020;144:72–8.
149. Uramoto H, Tanaka F. Recurrence after surgery in patients with NSCLC. Transl Lung Cancer Res. 2014;3(4):242–9.
150. Kirienko M, Cozzi L, Antunovic L, Lozza L, Fogliata A, Voulaz E, et al. Prediction of disease-free survival by the PET/CT radiomic signature in non-small cell lung cancer patients undergoing surgery. Eur J Nucl Med Mol Imaging. 2018;45(2):207–17.
151. Ciarmiello A, Giovannini E, Tutino F, Yosifov N, Milano A, Florimonte L et al. Does FDG PET-Based Radiomics have an added value for prediction of overall survival in Non-small Cell Lung Cancer? J Clin Med. 2024;13(9).
152. Rami-Porta R, Call S. Invasive staging of mediastinal lymph nodes: mediastinoscopy and remediastinoscopy. Thorac Surg Clin. 2012;22(2):177–89.
153. Tournoy KG, Keller SM, Annema JT. Mediastinal staging of lung cancer: novel concepts. Lancet Oncol. 2012;13(5):e221–9.
154. Gupta NC, Graeber GM, Bishop HA. Comparative efficacy of positron emission tomography with fluorodeoxyglucose in evaluation of small (< 1 cm), intermediate (1 to 3 cm), and large (> 3 cm) lymph node lesions. Chest. 2000;117(3):773–8.
155. Ouyang ML, Wang YR, Deng QS, Zhu YF, Zhao ZH, Wang L, et al. Development and validation of a (18)F-FDG PET-Based Radiomic Model for evaluating Hypermetabolic Mediastinal-Hilar Lymph nodes in Non-small-cell Lung Cancer. Front Oncol. 2021;11:710909.
156. Sepehri S, Tankyevych O, Upadhaya T, Visvikis D, Hatt M, Le Cheze C. Comparison and Fusion of Machine Learning Algorithms for Prospective Validation of PET/CT Radiomic Features Prognostic Value in Stage II-III Non-small Cell Lung Cancer. Diagnostics (Basel). 2021;11(4).
157. Lu LJ, Lv WB, Jiang J, Ma JH, Feng QJ, Rahmim A, et al. Robustness of Radiomic features in C-11 Choline and F-18 FDG PET/CT Imaging of Nasopharyngeal Carcinoma: impact of segmentation and discretization. Mol Imaging Biology. 2016;18(6):935–45.
158. Boellaard R. Standards for PET image acquisition and quantitative data analysis. J Nucl Med. 2009;50(Suppl 1):s11–20.
159. Carles M, Fechter T, Marti-Bonmati L, Baltas D, Mix M. Experimental phantom evaluation to identify robust positron emission tomography (PET) radiomic features. Ejnmmi Phys. 2021;8(1).
160. Anan N, Zainon R, Tamal M. A review on advances in F-18-FDG PET/CT radiomics standardisation and application in lung disease management. Insights into Imaging. 2022;13(1).
161. Boellaard R, Oyen WJ, Hoekstra CJ, Hoekstra OS, Visser EP, Willemsen AT, et al. The Netherlands protocol for standardisation and quantification of FDG whole body PET studies in multi-centre trials. Eur J Nucl Med Mol Imaging. 2008;35(12):2320–33.
162. Rizzo A, Triumbari EKA, Gatta R, Boldrini L, Racca M, Mayerhoefer M, et al. The role of F-18-FDG PET/CT radiomics in lymphoma. Clin Translational Imaging. 2021;9(6):589–98.
163. Raunig DL, McShane LM, Pennello G, Gatsonis C, Carson PL, Voyvodic JT, et al. Quantitative imaging biomarkers: a review of statistical methods for technical performance assessment. Stat Methods Med Res. 2015;24(1):27–67.
164. Da-Ano R, Visvikis D, Hatt M. Harmonization strategies for multicenter radiomics investigations. Phys Med Biol. 2020;65(24).
165. Collins GS, Reitsma JB, Altman DG, Moons KG. Transparent reporting of a multivariable prediction model for individual prognosis or diagnosis (TRIPOD): the TRIPOD statement. BMJ. 2015;350:g7594.
166. Guglielmo P, Marturano F, Bettinelli A, Gregianin M, Paiusco M, Evangelista L. Additional value of PET Radiomic features for the initial staging of prostate Cancer: a systematic review from the literature. Cancers. 2021;13:23.
167. Churchill IF, Sullivan KA, Simone AC, Patel YS, Leontiadis GI, Farrokhyar F, et al. Thoracic imaging radiomics for staging lung cancer: a systematic review and radiomic quality assessment. Clin Translational Imaging. 2022;10(2):191–216.
168. Spadarella G, Stanzione A, D'Antonoli TA, Andreychenko A, Fanni SC, Ugga L et al. Systematic review of the radiomics quality score applications: an EuSoMII Radiomics auditing Group Initiative. European Radiology.
169. Sanduleanu S, Woodruff HC, de Jong EEC, van Timmeren JE, Jochems A, Dubois L, et al. Tracking tumor biology with radiomics: a systematic review utilizing a radiomics quality score. Radiother Oncol. 2018;127(3):349–60.
170. Stanzione A, Gambardella M, Cuocolo R, Ponsiglione A, Romeo V, Imbriaco M. Prostate MRI radiomics: a systematic review and radiomic quality score assessment. Eur J Radiol. 2020;129.
171. Rogasch JMM, Shi K, Kersting D, Seifert R. Methodological evaluation of original articles on radiomics and machine learning for outcome prediction based on positron emission tomography (PET). Nuklearmedizin. 2023;62(6):361–9.
172. Currie G, Hawk KE, Rohren E, Vial A, Klein R. Machine Learning and Deep Learning in Medical Imaging: Intelligent Imaging. J Med Imaging Radiat Sci. 2019;50(4):477–87.
173. Avanzo M, Wei L, Stancanello J, Vallières M, Rao A, Morin O, et al. Machine and deep learning methods for radiomics. Med Phys. 2020;47(5):e185–202.
174. Duan WY, Xiong BD, Tian T, Zou XY, He ZN, Zhang L. Radiomics in Nasopharyngeal Carcinoma. Clin Med Insights-Oncology. 2022;16.
175. Gandhi Z, Gurram P, Amgai B, Lekkala SP, Lokhandwala A, Manne S et al. Artificial Intelligence and Lung Cancer: impact on improving patient outcomes. Cancers (Basel). 2023;15(21).

Publisher's note

Springer Nature remains neutral with regard to jurisdictional claims in published maps and institutional affiliations.